Hybrid high-order and weak Galerkin methods for the biharmonic problem

Zhaonan Dong, Alexandre Ern

Hybrid high-order and weak Galerkin methods for the biharmonic problem

Zhaonan Dong* Alexandre Ern†

April 8, 2022

Abstract

We devise and analyze two hybrid high-order (HHO) methods for the numerical approximation of the biharmonic problem. The methods support polyhedral meshes, rely on the primal formulation of the problem, and deliver $O(h^{k+1})$ H^2-error estimates when using polynomials of order $k \geq 0$ to approximate the normal derivative on the mesh (inter)faces. Both HHO methods hinge on a stabilization in the spirit of Lehrenfeld–Schöberl for second-order PDEs. The cell unknowns are polynomials of order $(k+2)$ that can be eliminated locally by means of static condensation. The face unknowns approximating the trace of the solution on the mesh (inter)faces are polynomials of order $(k+1)$ in the first HHO method which is valid in dimension two and uses an original stabilization involving the canonical hybrid finite element, and they are of order $(k+2)$ for the second HHO method which is valid in arbitrary dimension and uses only L^2-orthogonal projections in the stabilization. A comparative discussion with the weak Galerkin methods from the literature is provided, highlighting the close connections and the improvements proposed herein. Additionally, we show how the two HHO methods can be combined with a Nitsche-like boundary-penalty technique to weakly enforce the boundary conditions. An originality in the devised Nitsche's technique is to avoid any penalty parameter that must be large enough. Finally, numerical results showcase the efficiency of the proposed methods, and indicate that the HHO methods can generally outperform discontinuous Galerkin methods and even be competitive with C^0-interior penalty methods on triangular meshes.

1 Introduction

Fourth-order PDEs are encountered in the modeling of various physical phenomena, such as plate bending, thin-plate elasticity, microelectromechanical systems, and the Cahn–Hilliard phase-field model. In the present work, we are concerned with the following model problem:

$$\begin{aligned} \Delta^2 u &= f && \text{in } \Omega, \\ u &= 0 && \text{on } \partial\Omega, \\ \partial_n u &= 0 && \text{on } \partial\Omega, \end{aligned} \tag{1}$$

where Ω is an open, bounded, polytopal, Lipschitz set in $\mathbb{R}^d$, $d \geq 2$, with boundary $\partial\Omega$, the load f is in $L^2(\Omega)$, and ∂_n denotes the normal derivative on $\partial\Omega$. Non-homogeneous boundary conditions and a boundary condition on the second-normal derivative can be readily incorporated. Instead, considering more singular loads is nontrivial for the present purpose. We also emphasize that the present developments hinge on the weak formulation of (1) involving the Hessian.

The main goal of this work is to devise and analyze a discretization method for (1) offering two main features: (i) it supports polyhedral meshes (the mesh cells can be polyhedra as such or have a simple shape but contain hanging nodes); (ii) it hinges on the primal formulation of the problem, thereby leading to a symmetric positive definite system matrix. There are already some methods in the literature achieving these goals. These methods can be loosely classified into three groups, depending on

*Inria, 2 rue Simone Iff, 75589 Paris, France, and CERMICS, Ecole des Ponts, 77455 Marne-la-Vallée 2, France zhaonan.dong@inria.fr.

†CERMICS, Ecole des Ponts, 77455 Marne-la-Vallée 2, France, and Inria, 2 rue Simone Iff, 75589 Paris, France alexandre.ern@enpc.fr.

the dimension of the smallest geometric object to which discrete unknowns are attached. This criterion is relevant since it influences the stencil of the method, and it also influences the level of conformity that can be achieved in the approximation of the solution. The methods in the first group were developed in the practically important case where $d = 2$. They attach discrete unknowns to the mesh vertices, edges, and cells and can achieve C^1-conformity. Salient examples are the C^1-conforming virtual element methods (VEM) from [6, 13] and the C^0-conforming VEM from [50]. Another example of method in this group is the nonconforming VEM from [3, 51] where the approximation is, however, (fully) nonconforming. The methods in the second group attach discrete unknowns only to the mesh faces and cells for $d \geq 2$. They are amenable to static condensation (meaning that the cell unknowns can be eliminated locally leading to a global problem coupling only the face unknowns), and they provide a nonconforming approximation to the solution. The two salient examples are the weak Galerkin (WG) methods from [38, 49, 48] and the hybrid high-order (HHO) method from [4]. Finally, the methods in the third group attach discrete unknowns only to the mesh cells for $d \geq 2$ and belong to the class of interior penalty discontinuous Galerkin (IPDG) methods. These are also nonconforming methods, and they were developed for the model problem (1) in [37, 42, 31]. We mention that on specific meshes composed of simplices or cuboids, there are variants of the above methods achieving C^0-conformity, such as the C^0-WG method from [40, 12] and the C^0-IPDG from [25, 5]. Furthermore, important examples of nonconforming finite elements on simplicial meshes are the Morley element [36, 47] and the Hsieh–Clough–Tocher (HCT) element (see, e.g., [15, Chap. 6]).

In the present work, we focus on HHO methods. HHO methods were introduced in [21] for locking-free linear elasticity and in [22] for linear diffusion. The two ingredients of HHO methods are a local reconstruction operator and a local stabilization operator in each mesh cell. For second-order PDEs, the aim of the first operator is to reconstruct locally a gradient from the cell and the face unknowns, and the aim of the second operator is to penalize in a least-squares sense the difference between the trace of the cell unknown and the face unknown on every mesh face. HHO methods have undergone a vigorous development in the last few years; to cite a few examples, we mention Navier–Stokes flows [23], elastoplastic problems [2], Tresca friction problems [14], spectral problems [9], and magnetostatics [11]. HHO methods were embedded into the broad framework of hybridizable dG (HDG) methods in [17] by reformulating the HHO equations as local balance equations with equilibrated numerical fluxes. Moreover, HHO methods are closely related to WG methods, which were also embedded into the HDG framework in [16, Sec. 6.6]. The reconstruction operator in the HHO method corresponds to the weak gradient in WG methods. Hence, HHO and WG methods differ only in the choice of the discrete unknowns and in the design of stabilization. Although the close connections between HHO and WG methods should be mutually beneficial, these connections are, in the authors' opinion, not sufficiently explicit in the literature, and the title of the present work is also meant to draw the community's attention on this opportunity.

The design of the stabilization turns out to be a key ingredient so that the method leads to *optimal* error estimates. By this, we mean, in the case of a second-order elliptic PDE, that the method delivers an $O(h^{k+1})$ H^1-error estimate, where $k \geq 0$ is the degree of the face unknowns. Notice that this criterion is consistent with the classical properties of hybridized mixed finite element methods. The point we want to make here is that optimality cannot be reached on general meshes if one uses plain least-squares stabilization, i.e., a more subtle design of the stabilization is required. If the cell unknowns are of degree k, optimality is achieved in [21, 22] by means of a stabilization that uses the reconstruction operator (this is the first occurrence of this idea in the broad framework of HDG methods). Alternatively, if the cell unknowns are of degree $(k+1)$, one can use the Lehrenfeld–Schöberl (LS) stabilization [35], as in [17] for HHO methods and in [39] for WG methods. Although the LS stabilization does not use the reconstruction operator, it is not a plain least-squares stabilization, since an orthogonal projection is applied to the trace of the cell unknowns. We mention that it is also possible to achieve optimality *without stabilization* for second-order PDEs if one uses Raviart–Thomas functions of degree k to reconstruct the gradient (see [1, 19]). However, optimality is lost if one reconstructs the gradient in larger polynomial spaces (the convergence rate is in general $O(h^k)$), since the normal component of the reconstructed gradient on the mesh faces is too rich to be captured by the face unknowns. Another possibility is to enrich the space for the gradient reconstruction by suitable bubble functions based on the notion of M-decomposition devised for HDG methods [18].

To discretize fourth-order PDEs, HHO and WG methods use cell unknowns that are meant to approximate the solution in each mesh cell, face unknowns that are meant to approximate its trace on each mesh

unknowns	cell	face	grad	k	ref.
WG	$k+2$	$k+2$	$[k+1]^d$	$k \geq 0$	[38]
	$k+2$	$k+2$	$k+1$	$k \geq 0$	[38]
	$k+2$	$k+1$	$k+1$	$k \geq 0$	[49]
	1	1	$[1]^d$	$k = 0$	[48]
HHO	k	k	$[k]^d$	$k \geq 1$	[4]
HHO(A)	$k+2$	$k+1$	k	$k \geq 0$	present ($d = 2$)
HHO(B)	$k+2$	$k+2$	k	$k \geq 0$	present ($d \geq 2$)

Table 1: Discrete unknowns in HHO and WG methods from the literature and the present work. In the column 'grad', the notation $[\cdot]^d$ means that the full gradient is approximated; otherwise, only the normal derivative is approximated. For all the methods, the integer k is fixed by the fact that the method delivers an $O(h^{k+1})$ H^2-error estimate.

(inter)face, and additional face unknowns that are meant to approximate either its full gradient trace or only its normal derivative on each mesh (inter)face. The HHO and WG methods from the literature and the present HHO methods are described in Table 1 in terms of their discrete unknowns. To put all the methods on the same ground and allow for a fair comparison, the polynomial degree k is such that all the methods in the table deliver an $O(h^{k+1})$ H^2-error estimate. Consistently with the terminology adopted above for second-order elliptic PDEs, the method can be viewed as *optimal* if the order of the face unknowns approximating the trace of the gradient (or of the normal derivative) is of degree k. As seen from Table 1, the WG methods from the literature do not meet this criterion. For instance, the HHO method from [4] with $k = 1$ converges with one order higher than the WG method from [48] while using the same discrete unknowns. The lack of optimality is related to the use of a plain least-squares stabilization. Instead, the HHO method from [4] and the present HHO methods are optimal, and this is reflected by a more elaborate design of the stabilization. Notice that for fourth-order PDEs, this also means that the Hessian (and not only the Laplacian) has to be reconstructed locally. In [4], the stabilization design follows the spirit of [21, 22] in that it uses a Hessian-based deflection reconstruction operator. In the present methods, the design is performed in the spirit of the LS stabilization. Another difference with [4] is that the present methods only introduce face unknowns approximating the normal derivative of the solution on the mesh (inter)faces (and not the full gradient trace). As a result, and despite the slight increase in the degree of its face unknowns approximating the solution trace, the present HHO methods involve less globally coupled unknowns than in [4]; see the discussion in Remarks 3.1 and 5.2. Moreover, we allow here for $k \geq 0$, whereas [4] requires $k \geq 1$. We also mention that the increase of cell unknowns compared to [4] has a moderate impact on computational costs owing to static condensation. This slight overhead is actually compensated by the simplification in the stabilization term (see Section 7 for further discussion).

Let us briefly summarize the main novelties and results of the present work: (i) Two novel and computationally effective HHO methods leading to optimal $O(h^{k+1})$ H^2-error estimates with polynomials of order $k \geq 0$ to approximate the normal derivative; (ii) An original design in 2D using, for the first time in HHO methods, the canonical hybrid finite element in the stabilization; (iii) The HHO methods do not feature stabilization parameters that must be large enough (only positive), in contrast with dG and C^0-IPDG methods. (iv) A numerical study showing the attractive performances of the proposed methods, which in particular can outperform dG methods (except for low polynomial orders and Voronoi-like meshes where the number of faces is quite large) and even be competitive with C^0-IPDG and HCT methods on simplicial meshes; (v) A variant of the HHO methods using a Nitsche-type boundary-penalty technique to weakly enforce the boundary conditions. We notice in particular that the development of Nitsche's boundary-penalty technique is instrumental to deal with domains with curved boundary (in the wake of [8, 7] for elliptic interface problems) and to derive a robust approximation method in the case of singularly perturbed regimes. These results are explored in our recent work [24]. We also emphasize that our Nitsche technique does not need the penalty parameter to be large enough. This is the first time this property is met for fourth-order PDEs, and to this purpose, we adapt ideas from [34, 7] derived for second-order PDEs. Heuristically, the reason for circumventing the constraint on having a large enough penalty parameter is that the reconstruction operator in HHO methods avoids the need to introduce an

additional consistency term as in the standard Nitsche method.

As a final remark, we mention that our main error estimates are established for an exact solution that belongs to the broken Sobolev space $H^{k+3}(\mathcal{T}_h)$ (where $\mathcal{T}_h$ denotes the underlying mesh) and to the Sobolev space $H^{2+s}(\Omega)$ with $s > \frac{3}{2}$. This latter assumption follows the rather classical paradigm in the analysis of nonconforming methods and is invoked when bounding the consistency error. As discussed in Remark 4.7, the regularity gap can be lowered to $s > 1$ by adapting the techniques developed in [29] and [28, Chap. 40&41] in the context of second-order elliptic PDEs. We also notice that quasi-optimal error estimates for general loads in $H^{-2}(\Omega)$ are derived in [45, 44] for the Morley element and the C^0-IPDG method (see also [10] for further results in the case of various lowest-order methods). The techniques in [45, 44] require to modify the right-hand side of the discrete problem by means of bubble functions and a C^1-smoother. These ideas have been adapted to HHO methods for second-order elliptic PDEs with loads in $H^{-1}(\Omega)$ in [30]. We expect that the extension to the biharmonic problem could follow a similar path for $d = 2$, whereas for $d = 3$, one difficulty is related, irrespective of the considered discretization method, to the lack of a well-established and computable C^1-smoother of arbitrary order.

The rest of this work is organized as follows. We introduce some basic notation, the mesh assumptions, and some analysis tools in Section 2. In Section 3, we introduce the HHO method in the 2D setting employing the canonical hybrid finite element to design the stabilization. In Section 4, we present the stability and error analysis of the method introduced in Section 3. In Section 5, we present the second HHO method, this time valid in arbitrary dimension, and we outline the main changes in the stability and error analysis from Section 4. Our numerical results indicate that in two dimensions, the first HHO method from Section 3 is more effective than the second method from Section 5. In Section 6, we combine the above HHO methods with Nitsche's boundary-penalty technique. Finally, numerical results showcasing the computational advantages of the proposed HHO methods are presented in Section 7.

2 Model problem and discrete setting

In this section, we introduce some basic notation, the weak formulation of the model problem, and the discrete setting to formulate and analyze the HHO discretization.

2.1 Basic notation and weak formulation

We use standard notation for the Lebesgue and Sobolev spaces and, in particular, for the fractional-order Sobolev spaces, we consider the Sobolev–Slobodeckij seminorm based on the double integral. For an open, bounded, Lipschitz set S in $\mathbb{R}^d$, $d \in \{1, 2, 3\}$, we denote by $(v, w)_S$ the $L^2(S)$-inner product, and we employ the same notation when v and w are vector- or matrix-valued fields. We denote by ∇w the (weak) gradient of w and by $\nabla^2 w$ its (weak) Hessian. Let $\boldsymbol{n}$ be the unit outward normal vector on the boundary ∂S of S. Assuming that the functions v and w are smooth enough, we have the following integration by parts formula:

$$(\Delta^2 v, w)_S = (\nabla^2 v, \nabla^2 w)_S + (\nabla \Delta v, \boldsymbol{n} w)_{\partial S} - (\nabla^2 v \boldsymbol{n}, \nabla w)_{\partial S}. \tag{2}$$

Whenever the context is unambiguous, we denote by ∂_n the (scalar-valued) normal derivative on ∂S and by ∂_t the ($\mathbb{R}^{d-1}$-valued) tangential derivative. We also denote by $\partial_{nn} v$ the (scalar-valued) normal-normal second-order derivative and by $\partial_{nt} v$ the ($\mathbb{R}^{d-1}$-valued) normal-tangential second-order derivative. The integration by parts formula (2) can then be rewritten as

$$(\Delta^2 v, w)_S = (\nabla^2 v, \nabla^2 w)_S + (\partial_n \Delta v, w)_{\partial S} - (\partial_{nn} v, \partial_n w)_{\partial S} - (\partial_{nt} v, \partial_t w)_{\partial S}. \tag{3}$$

In what follows, the set S is always a polytope so that its boundary can be decomposed into a finite union of planar faces with disjoint interiors. Expressions involving the tangential derivative on ∂S are then implicitly understood to be evaluated as a summation over the faces composing ∂S.

Using the above integration by parts formula, the following weak formulation of the model problem (1) is classically derived: Find $u \in H^2_0(\Omega)$ such that

$$(\nabla^2 u, \nabla^2 v)_\Omega = (f, v)_\Omega, \qquad \forall v \in H^2_0(\Omega), \tag{4}$$

The well-posedness of (4) is proven, e.g., in [32, Section 1.5].

Remark 2.1 (Non-homogeneous conditions) *Since the domain Ω is a polytope, its boundary can be split into $\{\partial\Omega_i\}_{i=1}^N$ $(d-1)$-dimensional planar faces with disjoint interiors. Let g_D and g_N be boundary data such that $g_D|_{\partial\Omega_i} \in H^{\frac{3}{2}}(\partial\Omega_i)$ and $g_N|_{\partial\Omega_i} \in H^{\frac{1}{2}}(\partial\Omega_i)$ for all $i \in \{1,\dots,N\}$, as well as $g_D \in C^0(\partial\Omega)$. Then, one can enforce the non-homogeneous boundary conditions $u = g_D$ and $\partial_n u = g_N$ on all the faces $\partial\Omega_i$; see [33, Sections 1.5 &1.6].*

2.2 Inverse, trace, and Poincaré inequalities

Let $\mathcal{T}_h$ be a mesh covering Ω exactly. The mesh $\mathcal{T}_h$ can have cells that are disjoint open polytopes in $\mathbb{R}^d$ (with planar faces), and hanging nodes are possible. A generic mesh cell is denoted by $K \in \mathcal{T}_h$, its diameter by h_K, and its unit outward normal by $\boldsymbol{n}_K$. We assume that the mesh belongs to a shape-regular mesh sequence $(\mathcal{T}_h)_{h>0}$ in the sense of [21]. In a nutshell, any mesh $\mathcal{T}_h$ admits a matching simplicial submesh $\mathcal{T}_h'$ such that any cell (or face) of $\mathcal{T}_h'$ is a subset of exactly one cell (or at most one face) of $\mathcal{T}_h$. Moreover, there exists a mesh-regularity parameter $\rho > 0$ such that for all $h > 0$, all $K \in \mathcal{T}_h$, and all $S \in \mathcal{T}_h'$ such that $S \subset K$, we have $\rho h_S \le r_S$ and $\rho h_K \le h_S$, where r_S denotes the inradius of the simplex S. The mesh faces are collected in the set $\mathcal{F}_h$, which is split as the set $\mathcal{F}_h^{\mathrm{b}}$ containing the mesh boundary faces and the set $\mathcal{F}_h^{\mathrm{i}}$ containing the mesh interfaces. In this work, we make the mild additional assumption that the mesh faces are connected; the reason for this is that we will consider an approximation operator on the mesh faces that is only H^1-stable, and not L^2-stable, so that we will need to invoke some polynomial approximation properties directly on the mesh faces (see (14)). Let $\boldsymbol{n}_F$ denote the unit normal vector orienting any mesh face $F \in \mathcal{F}_h$. The direction of $\boldsymbol{n}_F$ is arbitrary, but fixed once and for all, for all $F \in \mathcal{F}_h^{\mathrm{i}}$, and $\boldsymbol{n}_F := \boldsymbol{n}$ for all $F \in \mathcal{F}_h^{\mathrm{b}}$. For any mesh cell $K \in \mathcal{T}_h$, the mesh faces composing its boundary ∂K are collected in the set $\mathcal{F}_{\partial K}$. The shape-regularity of the mesh sequence implies that for all $K \in \mathcal{T}_h$ and all $F \in \mathcal{F}_{\partial K}$ with diameter h_F, the length scales h_K and h_F are uniformly equivalent and that $\#(\mathcal{F}_{\partial K})$ is uniformly bounded.

Let us recall some important analysis tools. We refer the reader, e.g., to [20, Sec. 1.4] for the proofs of Lemma 2.2 and Lemma 2.3 and to [46] for the derivation of the Poincaré inequality in H^2 from the corresponding inequality in H^1. For all $K \in \mathcal{T}_h$ and all $k \ge 0$, $\mathbb{P}^k(K)$ denotes the linear space composed of the restriction to K of polynomials of total degree at most k.

Lemma 2.2 (Discrete inverse and trace inequalities) *Let $\mathcal{T}_h$ belong to a shape-regular mesh sequence and let $k \ge 0$. There are constants $C_{\mathrm{inv}}^{\mathrm{tr}}$ and C_{inv}, only depending on the mesh shape-regularity, the polynomial degree k, and the space dimension d, such that for all $v_h \in \mathbb{P}^k(K)$ and all $K \in \mathcal{T}_h$,*

$$\|v_h\|_{\partial K} \le C_{\mathrm{inv}}^{\mathrm{tr}} h_K^{-\frac{1}{2}} \|v_h\|_K, \tag{5}$$

$$\|\nabla v_h\|_K \le C_{\mathrm{inv}} h_K^{-1} \|v_h\|_K, \tag{6}$$

Lemma 2.3 (Multiplicative trace inequality) *Let $\mathcal{T}_h$ belong to a shape-regular mesh sequence. There is a constant C_{mt}, only depending on the mesh shape-regularity and the space dimension d, such that for all $v \in H^1(K)$ and all $K \in \mathcal{T}_h$,*

$$\|v\|_{\partial K} \le C_{\mathrm{mt}} \big(h_K^{-\frac{1}{2}} \|v\|_K + \|v\|_K^{\frac{1}{2}} \|\nabla v\|_K^{\frac{1}{2}} \big). \tag{7}$$

Lemma 2.4 (Poincaré inequality) *Let $\mathcal{T}_h$ belong to a shape-regular mesh sequence. There is a constant C_{P}, only depending on the mesh shape-regularity and the space dimension d, such that for all $v \in H^2(K)^\perp := \{v \in H^2(K) \mid (v,\xi)_K = 0,\ \forall \xi \in \mathbb{P}^1(K)\}$ and all $K \in \mathcal{T}_h$,*

$$h_K^{-2} \|v\|_K + h_K^{-1} \|\nabla v\|_K \le C_{\mathrm{P}} \|\nabla^2 v\|_K. \tag{8}$$

Remark 2.5 (Discrete inverse inequality on faces) *Similarly to (6) and recalling that the diameter of any face $F \in \mathcal{F}_{\partial K}$ is uniformly equivalent to h_K, one can prove that there is a constant $\widetilde{C}_{\mathrm{inv}}$, only depending on the mesh shape-regularity, the polynomial degree k, and the space dimension d, such that*

$$\|\partial_t v_h\|_F \le \widetilde{C}_{\mathrm{inv}} h_K^{-1} \|v_h\|_F, \tag{9}$$

for all $v_h \in \mathbb{P}^k(K)$, all $K \in \mathcal{T}_h$, and all $F \in \mathcal{F}_{\partial K}$.

Remark 2.6 (Fractional multiplicative trace inequality) *Let $\mathcal{T}_h$ belong to a shape-regular mesh sequence. Let $s \in (\frac{1}{2}, 1]$. There is a constant $C_{\rm fmt}$, only depending on the mesh shape-regularity and the space dimension d, such that for all $v \in H^s(K)$ and all $K \in \mathcal{T}_h$,*

$$\|v\|_{\partial K} \le C_{\rm fmt}\big(h_K^{-\frac{1}{2}}\|v\|_K + h_K^{s-\frac{1}{2}}|v|_{H^s(K)}\big). \tag{10}$$

The proof when K is a simplex can be found in [26, Lem. 7.2]. In the general case, for every subface of a face in $\mathcal{F}_{\partial K}$, one carves a subsimplex inside K whose height is uniformly equivalent to h_K. Notice that for $s = 1$, (10) is a simple consequence of (7) and Young's inequality since $|v|_{H^1(K)} = \|\nabla v\|_K$.

2.3 Polynomial approximation in cells and on faces

Let $k \ge 0$ and let Π_K^{k+2} be the L^2-orthogonal projection onto $\mathbb{P}^{k+2}(K)$. Since the mesh cells can be decomposed into a finite number of subsimplices, the approximation properties of Π_K^{k+2} can be established by proceeding as in [26, Lem. 5.4].

Lemma 2.7 (Polynomial approximation in K) *Let $\mathcal{T}_h$ belong to a shape-regular mesh sequence. Let $k \ge 0$. There is a constant $C_{\rm app}$, only depending on the mesh shape-regularity, the polynomial degree k, and the space dimension d, such that for all $t \in [0, k+3]$, all $m \in \{0, \dots, \lfloor t \rfloor\}$, all $v \in H^t(K)$, and all $K \in \mathcal{T}_h$,*

$$|v - \Pi_K^{k+2}(v)|_{H^m(K)} \le C_{\rm app} h_K^{t-m}|v|_{H^t(K)}. \tag{11}$$

Another useful property of Π_K^{k+2} results from the multiplicative trace inequality (7) and the Poincaré inequality (8). Indeed, we infer that there is a constant C_Π, only depending on the mesh shape-regularity, the polynomial degree k, and the space dimension d, such that for all $v \in H^2(K)$ and all $K \in \mathcal{T}_h$,

$$h_K^{-\frac{3}{2}}\|v - \Pi_K^{k+2}(v)\|_{\partial K} + h_K^{-\frac{1}{2}}\|\nabla(v - \Pi_K^{k+2}(v))\|_{\partial K} \le C_\Pi \|\nabla^2(v - \Pi_K^{k+2}(v))\|_K. \tag{12}$$

We will use two operators for the polynomial approximation on the mesh faces. The first one is an L^2-orthogonal projection. Specifically, letting $\mathbb{P}^k(\mathcal{F}_{\partial K}) := \times_{F\in\mathcal{F}_{\partial K}}\mathbb{P}^k(F)$ for all $k \ge 0$ and all $K \in \mathcal{T}_h$, we denote by $\Pi_{\partial K}^k$ the L^2-orthogonal projection onto $\mathbb{P}^k(\mathcal{F}_{\partial K})$. Notice that $\Pi_{\partial K}^k(v)$ can be computed independently for each face $F \in \mathcal{F}_{\partial K}$. The second operator is specific to the 2D setting where the mesh faces are straight segments. On the reference interval $\widehat{I} := (-1, 1)$, the canonical hybrid finite element of degree $(k+1)$ has for its degrees of freedom the value at the two endpoints and, for $k \ge 1$, the integrals on $\widehat{I}$ weighted by a chosen set of basis functions in $\mathbb{P}^{k-1}(\widehat{I})$ (see, e.g., [27, Sec. 6.3.3 & 7.6] or [41, Thm. 3.14]). For all $F \in \mathcal{F}_h$, let $J_F^{k+1} : H^1(F) \to \mathbb{P}^{k+1}(F)$ be the corresponding interpolation operator generated using geometric affine mappings. Then, the two key identities satisfied by J_F^{k+1} are for all $v \in H^1(F)$,

$$\big(\partial_t(v - J_F^{k+1}(v)), \xi\big)_F = 0,\ \forall \xi \in \mathbb{P}^k(F), \qquad (v - J_F^{k+1}(v), \theta)_F = 0,\ \forall \theta \in \mathbb{P}^{k-1}(F), \tag{13}$$

or, in more compact form, $\Pi_F^k(\partial_t v) = \partial_t(J_F^{k+1}(v))$ and $\Pi_F^{k-1} \circ J_F^{k+1} = \Pi_F^{k-1}$. Moreover, J_F^{k+1} satisfies the following approximation properties: There is C_J, only depending on the mesh shape-regularity, the polynomial degree k, and the space dimension d, such that

$$\|v - J_F^{k+1}(v)\|_F \le C_J h_F \|\partial_t v\|_F, \qquad \|v - J_F^{k+1}(v)\|_F \le C_J h_F^2 \|\partial_{tt} v\|_F, \tag{14}$$

for all $v \in H^1(F)$ and all $v \in H^2(F)$, respectively. Notice that for $k = 0$, J_F^1 coincides with the Lagrange interpolate on F based on its two endpoints.

In what follows, it is convenient to rewrite (13) and (14) on the whole boundary of every mesh cell $K \in \mathcal{T}_h$. Letting $H^l(\mathcal{F}_{\partial K}) := \{v \in L^2(\partial K) \mid v|_F \in H^l(F),\ \forall F \in \mathcal{F}_{\partial K}\}$ with $l \in \{1, 2\}$, $J_{\partial K}^{k+1} : H^1(\mathcal{F}_{\partial K}) \to \mathbb{P}^{k+1}(\mathcal{F}_{\partial K})$ is defined facewise by setting $J_{\partial K}^{k+1}(v)|_F := J_F^{k+1}(v|_F)$ for all $v \in H^1(\mathcal{F}_{\partial K})$. Recalling that the tangential derivative is understood to act facewise, we obtain for all $v \in H^1(\mathcal{F}_{\partial K})$,

$$\big(\partial_t(v - J_{\partial K}^{k+1}(v)), \xi\big)_{\partial K} = 0,\ \forall \xi \in \mathbb{P}^k(\mathcal{F}_{\partial K}), \qquad (v - J_{\partial K}^{k+1}(v), \theta)_{\partial K} = 0,\ \forall \theta \in \mathbb{P}^{k-1}(\mathcal{F}_{\partial K}). \tag{15}$$

Moreover, there is $\widetilde{C}_J$ having the same dependencies as C_J such that

$$\|v - J_{\partial K}^{k+1}(v)\|_{\partial K} \le \widetilde{C}_J h_K \|\partial_t v\|_{\partial K}, \qquad \|v - J_{\partial K}^{k+1}(v)\|_{\partial K} \le \widetilde{C}_J h_K^2 \|\partial_{tt} v\|_{\partial K}, \tag{16}$$

for all $v \in H^1(\mathcal{F}_{\partial K})$ and all $v \in H^2(\mathcal{F}_{\partial K})$, respectively, where we used that h_F and h_K are uniformly equivalent for all $F \in \mathcal{F}_{\partial K}$.

3 HHO method for the 2D biharmonic problem

Let $k \geq 0$ be the polynomial degree. For all $K \in \mathcal{T}_h$, the local HHO space is

$$\widehat{V}_K^k := \mathbb{P}^{k+2}(K) \times \mathbb{P}^{k+1}(\mathcal{F}_{\partial K}) \times \mathbb{P}^k(\mathcal{F}_{\partial K}). \tag{17}$$

A generic element in $\widehat{V}_K^k$ is denoted $\widehat{v}_K := (v_K, v_{\partial K}, \gamma_{\partial K})$ with $v_K \in \mathbb{P}^{k+2}(K)$, $v_{\partial K} \in \mathbb{P}^{k+1}(\mathcal{F}_{\partial K})$, and $\gamma_{\partial K} \in \mathbb{P}^k(\mathcal{F}_{\partial K})$. The first component of $\widehat{v}_K$ aims at representing the solution inside the mesh cell, the second its trace on the cell boundary, and the third its normal derivative on the cell boundary (along the direction of the outward normal $\boldsymbol{n}_K$). In what follows, it is implicitly understood that within integrals over ∂K, the symbol ∂_n means $\boldsymbol{n}_K \cdot \nabla$.

3.1 Reconstruction and stabilization

The HHO method is formulated locally by means of a reconstruction and a stabilization operator. The local reconstruction operator $R_K : \widehat{V}_K^k \to \mathbb{P}^{k+2}(K)$ is such that, for all $\widehat{v}_K := (v_K, v_{\partial K}, \gamma_{\partial K}) \in \widehat{V}_K^k$, $R_K(\widehat{v}_K) \in \mathbb{P}^{k+2}(K)$ is determined by solving the following well-posed problem:

$$\begin{aligned}(\nabla^2 R_K(\widehat{v}_K), \nabla^2 w)_K &= (\nabla^2 v_K, \nabla^2 w)_K + (v_K - v_{\partial K}, \partial_n \Delta w)_{\partial K} - (\partial_n v_K - \gamma_{\partial K}, \partial_{nn} w)_{\partial K} \\ &\quad - (\partial_t (v_K - v_{\partial K}), \partial_{nt} w)_{\partial K}, \quad \forall w \in \mathbb{P}^{k+2}(K), \\ (R_K(\widehat{v}_K), \xi)_K &= (v_K, \xi)_K, \quad \forall \xi \in \mathbb{P}^1(K).\end{aligned} \tag{18}$$

When computing $R_K(\widehat{v}_K)$, one actually takes $w \in \mathbb{P}^{k+2}(K)^\perp := \{w \in \mathbb{P}^{k+2}(K) \mid (w, \xi)_K = 0,\ \forall \xi \in \mathbb{P}^1(K)\}$ since the equation is trivial whenever $w \in \mathbb{P}^1(K)$. Moreover, owing to the integration by parts formula (3), we infer that

$$(\nabla^2 R_K(\widehat{v}_K), \nabla^2 w)_K = (v_K, \Delta^2 w)_K - (v_{\partial K}, \partial_n \Delta w)_{\partial K} + (\gamma_{\partial K}, \partial_{nn} w)_{\partial K} + (\partial_t v_{\partial K}, \partial_{nt} w)_{\partial K}. \tag{19}$$

This expression shows that in the rightmost term on the right-hand side, we take advantage of the face component $v_{\partial K}$ to represent the tangential derivative at the boundary of K. Notice also that for $k = 0$, the second term on the right-hand side vanishes.

The local stabilization bilinear form $S_{\partial K}$ is defined such that, for all $(\widehat{v}_K, \widehat{w}_K) \in \widehat{V}_K^k \times \widehat{V}_K^k$ with $\widehat{v}_K := (v_K, v_{\partial K}, \gamma_{\partial K})$ and $\widehat{w}_K := (w_K, w_{\partial K}, \chi_{\partial K})$,

$$\begin{aligned}S_{\partial K}(\widehat{v}_K, \widehat{w}_K) := {} & h_K^{-3} \big(J_{\partial K}^{k+1}(v_{\partial K} - v_K), J_{\partial K}^{k+1}(w_{\partial K} - w_K)\big)_{\partial K} \\ & + h_K^{-1} \big(\Pi_{\partial K}^k(\gamma_{\partial K} - \partial_n v_K), \Pi_{\partial K}^k(\chi_{\partial K} - \partial_n w_K)\big)_{\partial K}.\end{aligned} \tag{20}$$

Notice the use of the interpolation operator $J_{\partial K}^{k+1}$ for the first term on the right-hand side. The reconstruction and stabilization operators are combined together to build the local bilinear form a_K on $\widehat{V}_K^k \times \widehat{V}_K^k$ such that

$$a_K(\widehat{v}_K, \widehat{w}_K) := (\nabla^2 R_K(\widehat{v}_K), \nabla^2 R_K(\widehat{w}_K))_K + S_{\partial K}(\widehat{v}_K, \widehat{w}_K). \tag{21}$$

3.2 The global discrete problem

We define the global HHO space as

$$\widehat{V}_h^k := \mathbb{P}^{k+2}(\mathcal{T}_h) \times \mathbb{P}^{k+1}(\mathcal{F}_h) \times \mathbb{P}^k(\mathcal{F}_h). \tag{22}$$

A generic element in $\widehat{V}_h^k$ is denoted $\widehat{v}_h := (v_{\mathcal{T}_h}, v_{\mathcal{F}_h}, \gamma_{\mathcal{F}_h})$ with $v_{\mathcal{T}_h} := (v_K)_{K \in \mathcal{T}_h}$, $v_{\mathcal{F}_h} := (v_F)_{F \in \mathcal{F}_h}$, and $\gamma_{\mathcal{F}_h} := (\gamma_F)_{F \in \mathcal{F}_h}$, where γ_F is meant to approximate the normal derivative in the direction of the unit normal vector $\boldsymbol{n}_F$ orienting F. For all $K \in \mathcal{T}_h$, the local components of $\widehat{v}_h$ are collected in the triple $\widehat{v}_K := (v_K, v_{\partial K}, \gamma_{\partial K}) \in \widehat{V}_K^k$ with $v_{\partial K}|_F := v_F$ and $\gamma_{\partial K}|_F := (\boldsymbol{n}_F \cdot \boldsymbol{n}_K)\gamma_F$ for all $F \in \mathcal{F}_{\partial K}$. Notice that the way the face components of $v_{\partial K}$ are assigned follows the usual way of HHO methods for second-order elliptic PDEs, whereas the definition of the face components of $\gamma_{\partial K}$ takes into account the orientation of the faces in $\mathcal{F}_{\partial K}$. Furthermore, we enforce the homogeneous boundary conditions strongly by considering the subspace

$$\widehat{V}_{h0}^k := \{\widehat{v}_h \in \widehat{V}_h^k \mid v_F = \gamma_F = 0,\ \forall F \in \mathcal{F}_h^{\mathrm{b}}\}. \tag{23}$$

The discrete HHO problem for the 2D biharmonic problem is as follows: Find $\widehat{u}_h \in \widehat{V}_{h0}^k$ such that

$$a_h(\widehat{u}_h, \widehat{w}_h) = \ell(w_{\mathcal{T}_h}), \qquad \forall \widehat{w}_h \in \widehat{V}_{h0}^k, \tag{24}$$

where the global discrete bilinear form a_h and the global linear form ℓ are assembled cellwise as

$$a_h(\widehat{v}_h, \widehat{w}_h) := \sum_{K\in\mathcal{T}_h} a_K(\widehat{v}_K, \widehat{w}_K), \qquad \ell(w_{\mathcal{T}_h}) := (f, w_{\mathcal{T}_h})_\Omega = \sum_{K\in\mathcal{T}_h} (f, w_K)_K. \tag{25}$$

Notice that only the first component of the triple $\widehat{w}_h$ is used to evaluate the right-hand side in (24). An important observation is that the discrete problem (24) is amenable to static condensation. Indeed, the cell unknowns can be eliminated locally in every mesh cell, leading to a global problem where the only remaining unknowns are those attached to the mesh faces, i.e., those in $\mathbb{P}^{k+1}(\mathcal{F}_h) \times \mathbb{P}^k(\mathcal{F}_h)$.

Remark 3.1 (Comparison with [4]) *The present HHO method is cheaper than the one from [4] where the globally coupled unknowns are in $\mathbb{P}^k(\mathcal{F}_h) \times \mathbb{P}^k(\mathcal{F}_h;\mathbb{R}^2)$ with $k \geq 1$. Indeed, in the present method, there are $(2k+3)$, $k \geq 0$, unknowns per mesh interface, whereas this number is $(3k+3)$, $k \geq 1$, in [4]. On the other hand, the present method is slightly more expensive regarding static condensation since the number of cell unknowns is $\frac{1}{2}(k+3)(k+4)$ vs. $\frac{1}{2}(k+2)(k+3)$ in [4]. However, the slight overhead incurred in the static condensation is compensated by the simpler form of the stabilization; see Section 7 for more insight into the computational costs.*

Remark 3.2 (Variant) *It is also possible to consider the slightly cheaper choice $\widehat{V}_K^k := \mathbb{P}^{k+1}(K) \times \mathbb{P}^{k+1}(\partial K) \times \mathbb{P}^k(\partial K)$ with $k \geq 0$. With this choice, the number of cell unknowns to be statically condensed is slightly reduced, but the size of the global problem coupling all the face unknowns is unchanged. Notice that this choice requires to modify the stabilization bilinear form by setting*

$$\begin{aligned} S_{\partial K}(\widehat{v}_K, \widehat{w}_K) := {} & h_K^{-4}\big(\Pi_K^{k+1}(v_K - R_K(\widehat{v}_K)), \Pi_K^{k+1}(w_K - R_K(\widehat{w}_K))\big)_K \\ & + h_K^{-3}\big(J_{\partial K}^{k+1}(v_{\partial K} - R_K(\widehat{v}_K)), J_{\partial K}^{k+1}(w_{\partial K} - R_K(\widehat{w}_K))\big)_{\partial K} \\ & + h_K^{-1}\big(\Pi_{\partial K}^{k}(\gamma_{\partial K} - \partial_n R_K(\widehat{v}_K)), \Pi_{\partial K}^{k}(\chi_{\partial K} - \partial_n R_K(\widehat{w}_K))\big)_{\partial K}. \end{aligned} \tag{26}$$

The analysis of this variant will not be detailed herein, but this variant will be included in the numerical investigations presented in Section 7.

Remark 3.3 (Boundary conditions) *In the non-homogeneous case, the HHO solution is sought in the space $\widehat{V}_h^k$, whereas the test functions are still taken in the space $\widehat{V}_{h0}^k$. The value of the components of the HHO solution attached to the mesh boundary faces is then assigned by means of the projections $J_{\partial K}^{k+1}(g_D|_{\partial K})$ and $\Pi_{\partial K}^k(g_N|_{\partial K})$. The convergence analysis proceeds as for homogeneous boundary conditions, up to straightforward adaptations when bounding the consistency error. Details are omitted for brevity. It is also possible to consider the boundary conditions $u = \partial_{nn}u = 0$ on $\partial\Omega$. The discrete HHO bilinear form is still defined as above, but the discrete problem (24) now involves the subspace $\widehat{V}_{h0}^k := \{\widehat{v}_h \in \widehat{V}_h^k \mid v_F = 0,\ \forall F \in \mathcal{F}_h^{\mathrm{b}}\}$, i.e., the boundary condition $u = 0$ is still strongly enforced, whereas the boundary condition $\partial_{nn}u = 0$ is weakly enforced.*

4 Stability and error analysis

In this section, we perform the stability and error analysis of the HHO method devised in the previous section for the 2D biharmonic problem. We first establish a local stability property for the bilinear form a_K together with the well-posedness of the discrete problem (24). Then, we introduce a suitable reduction operator leading to optimal approximation properties, we bound the corresponding consistency error, and finally we derive the error estimate.

In what follows, the symbol C denotes a generic positive constant whose value can change at each occurrence, provided this value only depends on the mesh shape-regularity, the polynomial degree k, and the space dimension d.

4.1 Stability and well-posedness

We equip the local HHO space $\widehat{V}_K^k$ with the H^2-like seminorm such that for all $\widehat{v}_K := (v_K, v_{\partial K}, \gamma_{\partial K}) \in \widehat{V}_K^k$,

$$|\widehat{v}_K|_{\widehat{V}_K^k}^2 := \|\nabla^2 v_K\|_K^2 + h_K^{-3}\|v_{\partial K} - v_K\|_{\partial K}^2 + h_K^{-1}\|\gamma_{\partial K} - \partial_n v_K\|_{\partial K}^2. \tag{27}$$

Lemma 4.1 (Local stability and boundedness) *There is a real number $\alpha > 0$, depending only on the mesh shape-regularity, the polynomial degree k, and the space dimension d, such that for all $\widehat{v}_K \in \widehat{V}_K^k$ and all $K \in \mathcal{T}_h$,*

$$\alpha|\widehat{v}_K|_{\widehat{V}_K^k}^2 \le \|\nabla^2 R_K(\widehat{v}_K)\|_K^2 + S_{\partial K}(\widehat{v}_K, \widehat{v}_K) \le \alpha^{-1}|\widehat{v}_K|_{\widehat{V}_K^k}^2. \tag{28}$$

Proof. (1) Lower bound. Using the reconstruction defined in (18) with $w := v_K \in \mathbb{P}^{k+2}(K)$, we have

$$\begin{aligned}(\nabla^2 R_K(\widehat{v}_K), \nabla^2 v_K)_K &= \|\nabla^2 v_K\|_K^2 + (v_K - v_{\partial K}, \partial_n \Delta v_K)_{\partial K}\\ &\quad - (\partial_n v_K - \gamma_{\partial K}, \partial_{nn} v_K)_{\partial K} - (\partial_t(v_K - v_{\partial K}), \partial_{nt} v_K)_{\partial K}\\ &= \|\nabla^2 v_K\|_K^2 + (J_{\partial K}^{k+1}(v_K - v_{\partial K}), \partial_n \Delta v_K)_{\partial K}\\ &\quad - (\Pi_{\partial K}^k(\partial_n v_K - \gamma_{\partial K}), \partial_{nn} v_K)_{\partial K} - (\partial_t J_{\partial K}^{k+1}(v_K - v_{\partial K}), \partial_{nt} v_K)_{\partial K},\end{aligned} \tag{29}$$

where we used the two identities from (15) together with $\partial_n \Delta v_K \in \mathbb{P}^{k-1}(\mathcal{F}_{\partial K})$ (if $k \ge 1$, otherwise this term vanishes) and $\partial_{nn} v_K, \partial_{nt} v_K \in \mathbb{P}^k(\mathcal{F}_{\partial K})$. Using the Cauchy–Schwarz inequality together with the inverse inequalities (6), (5), and (9), we infer that

$$\begin{aligned}\|\nabla^2 v_K\|_K^2 &\le \|\nabla^2 R_K(\widehat{v}_K)\|_K\|\nabla^2 v_K\|_K + \|J_{\partial K}^{k+1}(v_K - v_{\partial K})\|_{\partial K}\|\partial_n \Delta v_K\|_{\partial K}\\ &\quad + \|\Pi_{\partial K}^k(\partial_n v_K - \gamma_{\partial K})\|_{\partial K}\|\partial_{nn} v_K\|_{\partial K} + \|\partial_t J_{\partial K}^{k+1}(v_K - v_{\partial K})\|_{\partial K}\|\partial_{nt} v_K\|_{\partial K}\\ &\le \|\nabla^2 R_K(\widehat{v}_K)\|_K\|\nabla^2 v_K\|_K + C S_{\partial K}(\widehat{v}_K, \widehat{v}_K)^{\frac12}\|\nabla^2 v_K\|_K,\end{aligned}$$

which shows that

$$\|\nabla^2 v_K\|_K \le \|\nabla^2 R_K(\widehat{v}_K)\|_K + C S_{\partial K}(\widehat{v}_K, \widehat{v}_K)^{\frac12}. \tag{30}$$

Moreover, since $v_{\partial K} - v_K = J_{\partial K}^{k+1}(v_{\partial K} - v_K) - (v_K - J_{\partial K}^{k+1}(v_K))$, the triangle inequality implies that

$$\begin{aligned}h_K^{-\frac32}\|v_{\partial K} - v_K\|_{\partial K} &\le h_K^{-\frac32}\|J_{\partial K}^{k+1}(v_{\partial K} - v_K)\|_{\partial K} + h_K^{-\frac32}\|v_K - J_{\partial K}^{k+1}(v_K)\|_{\partial K}\\ &\le S_{\partial K}(\widehat{v}_K, \widehat{v}_K)^{\frac12} + C h_K^{\frac12}\|\partial_{tt} v_K\|_{\partial K}\\ &\le S_{\partial K}(\widehat{v}_K, \widehat{v}_K)^{\frac12} + C\|\nabla^2 v_K\|_K,\end{aligned}$$

where we used the approximation property (16) and the discrete trace inequality (5). Combining this bound with (30) proves that

$$h_K^{-\frac32}\|v_{\partial K} - v_K\|_{\partial K} \le C\big(\|\nabla^2 R_K(\widehat{v}_K)\|_K + S_{\partial K}(\widehat{v}_K, \widehat{v}_K)^{\frac12}\big). \tag{31}$$

Proceeding similarly shows that

$$\begin{aligned}h_K^{-\frac12}\|\gamma_{\partial K} - \partial_n v_K\|_{\partial K} &\le h_K^{-\frac12}\|\Pi_{\partial K}^k(\gamma_{\partial K} - \partial_n v_K)\|_{\partial K} + h_K^{-\frac12}\|\partial_n v_K - \Pi_{\partial K}^k(\partial_n v_K)\|_{\partial K}\\ &\le S_{\partial K}(\widehat{v}_K, \widehat{v}_K)^{\frac12} + C h_K^{\frac12}\|\partial_{nt} v_K\|_{\partial K}\\ &\le S_{\partial K}(\widehat{v}_K, \widehat{v}_K)^{\frac12} + C\|\nabla^2 v_K\|_K,\end{aligned}$$

where we used the approximation properties of $\Pi_{\partial K}^k$ and the discrete trace inequality (5). Combining this bound with (30) proves that

$$h_K^{-\frac12}\|\gamma_{\partial K} - \partial_n v_K\|_{\partial K} \le C\big(\|\nabla^2 R_K(\widehat{v}_K)\|_K + S_{\partial K}(\widehat{v}_K, \widehat{v}_K)^{\frac12}\big). \tag{32}$$

Finally, combining the bounds (30), (31), and (32) proves the lower bound in (28).
(2) Upper bound. Using this time $w := R_K(\widehat{v}_K) \in \mathbb{P}^{k+2}(K)$ in the reconstruction defined in (18) and proceeding as above shows that

$$\|\nabla^2 R_K(\widehat{v}_K)\|_K \le \|\nabla^2 v_K\|_K + C S_{\partial K}(\widehat{v}_K, \widehat{v}_K)^{\frac12}. \tag{33}$$

Moreover, still proceeding as above, we infer that

$$\begin{aligned} h_K^{-\frac{3}{2}}\|J_{\partial K}^{k+1}(v_{\partial K}-v_K)\|_{\partial K} &\le h_K^{-\frac{3}{2}}\|v_{\partial K}-v_K\|_{\partial K}+h_K^{-\frac{3}{2}}\|v_K-J_{\partial K}^{k+1}(v_K)\|_{\partial K}\\ &\le h_K^{-\frac{3}{2}}\|v_{\partial K}-v_K\|_{\partial K}+C\|\nabla^2 v_K\|_K, \end{aligned}$$

and

$$h_K^{-\frac{1}{2}}\|\Pi_{\partial K}^k(\gamma_{\partial K}-\partial_n v_K)\|_{\partial K} \le h_K^{-\frac{1}{2}}\|\gamma_{\partial K}-\partial_n v_K\|_{\partial K}+C\|\nabla^2 v_K\|_K.$$

Putting the above two bounds together shows that

$$S_{\partial K}(\widehat{v}_K,\widehat{v}_K)^{\frac{1}{2}} \le C|\widehat{v}_K|_{\widehat{V}_K^k}. \tag{34}$$

Finally, the combination of (33) and (34) proves the upper bound in (28). □

We equip the space $\widehat{V}_{h0}^k$ with the norm

$$\|\widehat{v}_h\|_{\widehat{V}_{h0}^k} := \sum_{K\in\mathcal{T}_h}|\widehat{v}_K|_{\widehat{V}_K^k}^2, \qquad \forall \widehat{v}_h\in\widehat{V}_{h0}^k. \tag{35}$$

To show that this indeed defines a norm, consider $\widehat{v}_h\in\widehat{V}_{h0}^k$ such that $\|\widehat{v}_h\|_{\widehat{V}_{h0}^k}=0$. Then, for all $K\in\mathcal{T}_h$, $v_K\in\mathbb{P}^1(K)$ and $v_{\partial K}=v_K$ and $\gamma_{\partial K}=\partial_n v_K$ on ∂K. For any cell $K\in\mathcal{T}_h$ having at least one boundary face, say $F\in\mathcal{F}_{\partial K}\cap\mathcal{F}_h^{\rm b}$, we have $v_F=\gamma_F=0$ by definition of $\widehat{V}_{h0}^k$. Since v_K is affine and its gradient vanishes identically on F, ∇v_K vanishes in K, and since v_K vanishes on F, we infer that v_K vanishes identically in K. This implies that $v_F=\gamma_F=0$ for all $F\in\mathcal{F}_{\partial K}$. We can then propagate the reasoning one layer of cells further inside the domain, and by repeating the process, we reach all the cells composing the mesh. Thus, the three components of the triple $\widehat{v}_h$ vanish identically everywhere.

Corollary 4.2 (Coercivity and well-posedness) *The discrete bilinear form a_h is coercive on $\widehat{V}_{h0}^k$, and the discrete problem (24) is well-posed.*

Proof. Summing the lower bound in (28) over all the mesh cells shows the following coercivity property:

$$a_h(\widehat{v}_h,\widehat{v}_h)\ge\alpha\|\widehat{v}_h\|_{\widehat{V}_{h0}^k}^2, \qquad \forall\widehat{v}_h\in\widehat{V}_{h0}^k. \tag{36}$$

The well-posedness of (24) then follows from the Lax–Milgram lemma. □

4.2 Local reduction operator and polynomial approximation

For all $K\in\mathcal{T}_h$, we define the local reduction operator $\widehat{\mathcal{I}}_K^k : H^2(K)\to\widehat{V}_K^k$ such that for all $v\in H^2(K)$,

$$\widehat{\mathcal{I}}_K^k(v) := \big(\Pi_K^{k+2}(v), J_{\partial K}^{k+1}(v), \Pi_{\partial K}^k(\boldsymbol{n}_K\cdot\nabla v)\big)\in\widehat{V}_K^k. \tag{37}$$

Moreover, the H^2-elliptic projection $\mathcal{E}_K(v) : H^2(K)\to\mathbb{P}^{k+2}(K)$ is defined such that

$$\begin{aligned} (\nabla^2(\mathcal{E}_K(v)-v),\nabla^2 w)_K &= 0, \qquad \forall w\in\mathbb{P}^{k+2}(K),\\ (\mathcal{E}_K(v)-v,\xi)_K &= 0, \qquad \forall\xi\in\mathbb{P}^1(K). \end{aligned} \tag{38}$$

The following lemma states the two key properties of the local reduction operator defined in (37).

Lemma 4.3 (Local reduction operator) *We have $R_K\circ\widehat{\mathcal{I}}_K^k=\mathcal{E}_K$ for all $K\in\mathcal{T}_h$. Moreover, for all $K\in\mathcal{T}_h$ and all $v\in H^2(K)$, we have*

$$S_{\partial K}(\widehat{\mathcal{I}}_K^k(v),\widehat{\mathcal{I}}_K^k(v))^{\frac{1}{2}} \le C\|\nabla^2(v-\Pi_K^{k+2}(v))\|_K. \tag{39}$$

Proof. Let $K \in \mathcal{T}_h$ and let $v \in H^2(K)$.
(1) Using the definition (19) of the reconstruction operator, we infer that for all $w \in \mathbb{P}^{k+2}(K)$, we have

$$(\nabla^2 R_K(\widehat{\mathcal{I}}_K^k(v)), \nabla^2 w)_K = (\Pi_K^{k+2}(v), \Delta^2 w)_K \\ - (J_{\partial K}^{k+1}(v), \partial_n \Delta w)_{\partial K} + (\Pi_{\partial K}^k(\partial_n v), \partial_{nn} w)_{\partial K} + (\partial_t(J_{\partial K}^{k+1}(v)), \partial_{nt} w)_{\partial K}.$$

Since $\Delta^2 w \in \mathbb{P}^{k-2}(K)$ for $k \geq 2$ (and vanishes otherwise), $\partial_n \Delta w \in \mathbb{P}^{k-1}(K)$ for $k \geq 1$ (and vanishes otherwise), $\partial_{nn} w \in \mathbb{P}^k(K)$, and $\partial_{nt} w \in \mathbb{P}^k(K)$, the L^2-orthogonality properties of Π_K^{k+2} and $\Pi_{\partial K}^k$, together with the identities (15) satisfied by $J_{\partial K}^{k+1}$ imply that

$$(\nabla^2 R_K(\widehat{\mathcal{I}}_K^k(v)), \nabla^2 w)_K = (v, \Delta^2 w)_K - (v, \partial_n \Delta w)_{\partial K} + (\partial_n v, \partial_{nn} w)_{\partial K} + (\partial_t v, \partial_{nt} w)_{\partial K} = (\nabla^2 v, \nabla^2 w)_K.$$

Moreover, for all $\xi \in \mathbb{P}^1(K)$, we have $(R_K(\widehat{\mathcal{I}}_K^k(v)), \xi)_K = (\Pi_K^{k+2}(v), \xi)_K = (v, \xi)_K$ for all $\xi \in \mathbb{P}_1(K)$. The above two identities prove that $R_K(\widehat{\mathcal{I}}_K^k(v)) = \mathcal{E}_K(v)$ for all $v \in H^2(K)$. Thus, $R_K \circ \widehat{\mathcal{I}}_K^k = \mathcal{E}_K$.
(2) Let us now prove (39). Recalling the definitions (20) and (37), we have

$$S_{\partial K}(\widehat{\mathcal{I}}_K^k(v), \widehat{\mathcal{I}}_K^k(v))^{\frac{1}{2}} \leq h_K^{-\frac{3}{2}} \|J_{\partial K}^{k+1}(v - \Pi_K^{k+2}(v))\|_{\partial K} + h_K^{-\frac{1}{2}} \|\Pi_{\partial K}^k(\partial_n v - \partial_n \Pi_K^{k+2}(v))\|_{\partial K}, \tag{40}$$

where we used that $J_{\partial K}^{k+1} \circ J_{\partial K}^{k+1} = J_{\partial K}^{k+1}$ and $\Pi_{\partial K}^k \circ \Pi_{\partial K}^k = \Pi_{\partial K}^k$. We start with the first term in (40) where we set $\phi := v - \Pi_K^{k+2}(v)$. Notice that $\phi \in H^2(K)^\perp$ and that $\phi|_{\partial K} \in H^1(\mathcal{F}_{\partial K})$. Invoking the triangle inequality, the approximation property (16), and the trace inequality (12) shows that

$$h_K^{-\frac{3}{2}} \|J_{\partial K}^{k+1}(\phi)\|_{\partial K} \leq h_K^{-\frac{3}{2}} \|\phi\|_{\partial K} + h_K^{-\frac{3}{2}} \|\phi - J_{\partial K}^{k+1}(\phi)\|_{\partial K} \\ \leq h_K^{-\frac{3}{2}} \|\phi\|_{\partial K} + C h_K^{-\frac{1}{2}} \|\partial_t \phi\|_{\partial K} \leq C \|\nabla^2 \phi\|_K = C \|\nabla^2 (v - \Pi_K^{k+2}(v))\|_K.$$

Moreover, for the second term in (40), we invoke the $L^2(\partial K)$-stability of $\Pi_{\partial K}^k$ and the trace inequality (12) to show that

$$h_K^{-\frac{1}{2}} \|\Pi_{\partial K}^k(\partial_n v - \partial_n(\Pi_K^{k+2}(v))\|_{\partial K} \leq h_K^{-\frac{1}{2}} \|\partial_n(v - \Pi_K^{k+2}(v))\|_{\partial K} \leq C \|\nabla^2(v - \Pi_K^{k+2}(v))\|_K.$$

Combining the above two bounds with (40) proves (39). □

To bound the consistency error in the next section, we will consider a norm that is stronger than the H^2-norm. For all $K \in \mathcal{T}_h$ and all $v \in H^{2+s}(K)$, $s > \frac{3}{2}$, we consider the following norm:

$$\|v\|_{\sharp,K}^2 := \|\nabla^2 v\|_K^2 + h_K^3 \|\partial_n \Delta v\|_{\partial K}^2 + h_K \|\partial_{nn} v\|_{\partial K}^2 + h_K \|\partial_{nt} v\|_{\partial K}^2. \tag{41}$$

Lemma 4.4 (Approximation) *The following holds true for all $K \in \mathcal{T}_h$ and all $v \in H^{2+s}(K)$, $s > \frac{3}{2}$:*

$$\|v - \mathcal{E}_K(v)\|_{\sharp,K} \leq C \|v - \Pi_K^{k+2}(v)\|_{\sharp,K}. \tag{42}$$

Proof. Using the triangle inequality, we have

$$\|v - \mathcal{E}_K(v)\|_{\sharp,K} \leq \|v - \Pi_K^{k+2}(v)\|_{\sharp,K} + \|\mathcal{E}_K(v) - \Pi_K^{k+2}(v)\|_{\sharp,K},$$

so that we only need to bound the second term on the right-hand side. Owing to the discrete inverse and trace inequalities (5) and (6), we readily infer that

$$\|\mathcal{E}_K(v) - \Pi_K^{k+2}(v)\|_{\sharp,K} \leq C \|\nabla^2(\mathcal{E}_K(v) - \Pi_K^{k+2}(v))\|_K,$$

so that it remains to bound $\|\nabla^2(\mathcal{E}_K(v) - \Pi_K^{k+2}(v))\|_K$. Recalling that $\mathcal{E}_K = R_K \circ \widehat{\mathcal{I}}_K^k$, using the definition (18) of the reconstruction operator, and reasoning as in the proof of Lemma 4.3 to remove the various projection operators, we infer that

$$(\nabla^2 \mathcal{E}_K(v), \nabla^2 w)_K = (\nabla^2 \Pi_K^{k+2}(v), \nabla^2 w)_K + (\Pi_K^{k+2}(v) - v, \partial_n \Delta w)_{\partial K} \\ - (\partial_n(\Pi_K^{k+2}(v) - v), \partial_{nn} w)_{\partial K} - (\partial_t(\Pi_K^{k+2}(v) - v), \partial_{nt} w)_{\partial K},$$

for all $w \in \mathbb{P}^{k+2}(K)$. Taking $w := \mathcal{E}_K(v) - \Pi_K^{k+2}(v)$, and invoking the Cauchy–Schwarz inequality together with the discrete trace and inverse inequalities (5) and (6), we infer that

$$\|\nabla^2(\mathcal{E}_K(v) - \Pi_K^{k+2}(v))\|_K \leq C\big(h_K^{-\frac{3}{2}} \|v - \Pi_K^{k+2}(v)\|_{\partial K} + h_K^{-\frac{1}{2}} \|\nabla(v - \Pi_K^{k+2}(v))\|_{\partial K}\big) \\ \leq C \|\nabla^2(v - \Pi_K^{k+2}(v))\|_K,$$

where the last bound follows from the trace inequality (12). This completes the proof. □

4.3 Bound on consistency error

The global reduction operator $\widehat{\mathcal{I}}_h^k : H^2(\Omega) \to \widehat{V}_h^k$ is defined such that for all $v \in H^2(\Omega)$,

$$\widehat{\mathcal{I}}_h^k(v) := \big((\Pi_K^{k+2}(v))_{K\in\mathcal{T}_h}, (J_F^{k+1}(v))_{F\in\mathcal{F}_h}, (\Pi_F^k(\boldsymbol{n}_F\cdot\nabla v))_{F\in\mathcal{F}_h}\big) \in \widehat{V}_h^k, \tag{43}$$

recalling that v and ∇v are single-valued on every $F \in \mathcal{F}_h^{\mathrm{i}}$ for all $v \in H^2(\Omega)$. Importantly, we notice that for all $K \in \mathcal{T}_h$, the local components of $\widehat{\mathcal{I}}_h^k(v)$ attached to K and the faces composing its boundary are $\widehat{\mathcal{I}}_K^k(v|_K)$. Moreover, for the exact solution u of (4), we have $\widehat{\mathcal{I}}_h^k(u) \in \widehat{V}_{h0}^k$. We define the consistency error $\delta_h \in (\widehat{V}_{h0}^k)'$ such that

$$\langle \delta_h, \widehat{w}_h\rangle := \ell(w_{\mathcal{T}_h}) - a_h(\widehat{\mathcal{I}}_h^k(u), \widehat{w}_h), \qquad \forall \widehat{w}_h \in \widehat{V}_{h0}^k, \tag{44}$$

where $\langle\cdot,\cdot\rangle$ denotes the duality pairing between $(\widehat{V}_{h0}^k)'$ and $\widehat{V}_{h0}^k$.

Lemma 4.5 (Consistency) *Assume that $u \in H^{2+s}(\Omega)$ with $s > \frac{3}{2}$. The following holds true:*

$$\|\delta_h\|_{(\widehat{V}_{h0}^k)'} := \sup_{\widehat{w}_h\in\widehat{V}_{h0}^k} \frac{|\langle\delta_h,\widehat{w}_h\rangle|}{\|\widehat{w}_h\|_{\widehat{V}_{h0}^k}} \le C\left(\sum_{K\in\mathcal{T}_h} \|u - \Pi_K^{k+2}(u)\|_{\sharp,K}^2\right)^{\frac12}. \tag{45}$$

Proof. Let $\widehat{w}_h \in \widehat{V}_{h0}^k$. Using the definition of ℓ in (25), the PDE and the boundary conditions satisfied by the exact solution u, and integrating by parts cellwise, we infer that

$$\ell(w_{\mathcal{T}_h}) = \sum_{K\in\mathcal{T}_h}\Big\{(\nabla^2 u, \nabla^2 w_K)_K + (\partial_n\Delta u, w_K)_{\partial K} - (\partial_{nn}u, \partial_n w_K)_{\partial K} - (\partial_{nt}u, \partial_t w_K)_{\partial K}\Big\}.$$

The assumption $u \in H^{2+s}(\Omega)$ with $s > \frac{3}{2}$ implies that $(\partial_n\Delta u)|_{\partial K}$, $(\partial_{nn}u)|_{\partial K}$, and $(\partial_{nt}u)|_{\partial K}$ are meaningful in $L^2(\partial K)$ and single-valued at every mesh interface. Moreover, since $w_{\partial K}$, $\partial_t w_{\partial K}$, and $\chi_{\partial K}$ are single-valued at every mesh interface $\mathcal{F}_h^{\mathrm{i}}$ and vanish at each mesh boundary face since $\widehat{w}_h \in \widehat{V}_{h0}^k$, we have

$$\begin{aligned}\ell(w_{\mathcal{T}_h}) = \sum_{K\in\mathcal{T}_h}\Big\{&(\nabla^2 u, \nabla^2 w_K)_K + (\partial_n\Delta u, w_K - w_{\partial K})_{\partial K}\\ &- (\partial_{nn}u, \partial_n w_K - \chi_{\partial K})_{\partial K} - (\partial_{nt}u, \partial_t(w_K - w_{\partial K}))_{\partial K}\Big\}.\end{aligned}$$

Since a_h is assembled cellwise (see (25)) and the local components of $\widehat{\mathcal{I}}_h^k(u)$ are $\widehat{\mathcal{I}}_K^k(u|_K)$ for all $K \in \mathcal{T}_h$, we infer that $a_h(\widehat{\mathcal{I}}_h^k(u), \widehat{w}_h) = \sum_{K\in\mathcal{T}_h} a_K(\widehat{\mathcal{I}}_K^k(u|_K), \widehat{w}_K)$. Using the definition (21) of a_K, the definition (18) of $R_K(\widehat{w}_K)$, and the identity $R_K \circ \widehat{\mathcal{I}}_K^k = \mathcal{E}_K$ from Lemma 4.3 leads to

$$\begin{aligned}a_h(\widehat{\mathcal{I}}_h^k(u), \widehat{w}_h) = \sum_{K\in\mathcal{T}_h}\Big\{&(\nabla^2\mathcal{E}_K(u), \nabla^2 w_K)_K + (\partial_n\Delta\mathcal{E}_K(u), w_K - w_{\partial K})_{\partial K}\\ &- (\partial_{nn}\mathcal{E}_K(u), \partial_n w_K - \chi_{\partial K})_{\partial K} - (\partial_{nt}\mathcal{E}_K(u), \partial_t(w_K - w_{\partial K}))_{\partial K} + S_{\partial K}(\widehat{\mathcal{I}}_K^k(u), \widehat{w}_K)\Big\}.\end{aligned}$$

Defining the function η cellwise as $\eta|_K := u|_K - \mathcal{E}_K(u|_K)$ for all $K \in \mathcal{T}_h$, we infer that

$$\begin{aligned}\langle\delta_h, \widehat{w}_h\rangle = \sum_{K\in\mathcal{T}_h}\Big\{&(\nabla^2\eta, \nabla^2 w_K)_K + (\partial_n\Delta\eta, w_K - w_{\partial K})_{\partial K}\\ &- (\partial_{nn}\eta, \partial_n w_K - \chi_{\partial K})_{\partial K} - (\partial_{nt}\eta, \partial_t(w_K - w_{\partial K}))_{\partial K} - S_{\partial K}(\widehat{\mathcal{I}}_K^k(u), \widehat{w}_K)\Big\}.\end{aligned} \tag{46}$$

(Notice that $(\nabla^2\eta, \nabla^2 w_K)_K = 0$, but we keep this term since it can be bounded as the other ones.) Let us denote by $\mathcal{T}_{1,K}$ the first four addends on the right-hand side and by $\mathcal{T}_{2,K}$ the fifth addend. We bound $\mathcal{T}_{1,K}$ by the Cauchy–Schwarz inequality and also invoke the inverse inequality (9). Recalling the definition (41) of the $\|\cdot\|_{\sharp,K}$-norm, this yields

$$|\mathcal{T}_{1,K}| \le C\|\eta\|_{\sharp,K}|\widehat{w}_K|_{\widehat{V}_K^k}.$$

Moreover, owing to (39) and the upper bound in (28), we have

$$|\mathcal{T}_{2,K}| \le S_{\partial K}(\widehat{\mathcal{I}}_K^k(u),\widehat{\mathcal{I}}_K^k(u))^{\frac12} S_{\partial K}(\widehat{w}_K,\widehat{w}_K)^{\frac12} \le C\|\nabla^2(u-\Pi_K^{k+2}(u))\|_K |\widehat{w}_K|_{\widehat{V}_K^k}.$$

Altogether, this implies that

$$|\langle \delta_h, \widehat{w}_h\rangle| \le C\left(\sum_{K\in\mathcal{T}_h} \|\eta\|_{\sharp,K}^2 + \|\nabla^2(u-\Pi_K^{k+2}(u))\|_K^2\right)^{\frac12} \|\widehat{w}_h\|_{\widehat{V}_{h0}^k}.$$

Invoking Lemma 4.4, this completes the proof. □

4.4 Error estimate

We are now ready to establish the main result concerning the error analysis.

Theorem 4.6 (H^2-error estimate) *Assume that $u \in H^{2+s}(\Omega)$ with $s > \frac12$. The following holds true:*

$$\sum_{K\in\mathcal{T}_h} \|\nabla^2(u-R_K(\widehat{u}_K))\|_K^2 \le C \sum_{K\in\mathcal{T}_h} \|u-\Pi_K^{k+2}(u)\|_{\sharp,K}^2. \tag{47}$$

Consequently, if $k \ge 1$, assuming $u|_K \in H^{k+3}(K)$ for all $K \in \mathcal{T}_h$, we have

$$\sum_{K\in\mathcal{T}_h} \|\nabla^2(u-R_K(\widehat{u}_K))\|_K^2 \le C \sum_{K\in\mathcal{T}_h} \left(h_K^{k+1}|u|_{H^{k+3}(K)}\right)^2, \tag{48}$$

and if $k = 0$, letting $\sigma := \min(s-1,1) \in (\frac12, 1]$, we have

$$\sum_{K\in\mathcal{T}_h} \|\nabla^2(u-R_K(\widehat{u}_K))\|_K^2 \le C \sum_{K\in\mathcal{T}_h} \left(h_K(|u|_{H^3(K)} + h_K^\sigma |u|_{H^{3+\sigma}(K)})\right)^2. \tag{49}$$

Proof. Set $\widehat{e}_h := \widehat{\mathcal{I}}_h^k(u) - \widehat{u}_h \in \widehat{V}_{h0}^k$, so that $a_h(\widehat{e}_h,\widehat{e}_h) = -\langle \delta_h, \widehat{e}_h\rangle$. The coercivity property (36) implies that

$$\alpha\|\widehat{e}_h\|_{\widehat{V}_{h0}^k}^2 \le a_h(\widehat{e}_h,\widehat{e}_h) = -\langle \delta_h,\widehat{e}_h\rangle \le \|\delta_h\|_{(\widehat{V}_{h0}^k)'}\|\widehat{e}_h\|_{\widehat{V}_{h0}^k},$$

so that $\|\widehat{e}_h\|_{\widehat{V}_{h0}^k} \le \frac1\alpha\|\delta_h\|_{(\widehat{V}_{h0}^k)'}$. Since $\sum_{K\in\mathcal{T}_h}\|\nabla^2 R_K(\widehat{e}_K)\|_K^2 \le C\|\widehat{e}_h\|_{\widehat{V}_{h0}^k}^2$, we infer from Lemma 4.5 that

$$\sum_{K\in\mathcal{T}_h} \|\nabla^2 R_K(\widehat{e}_K)\|_K^2 \le C \sum_{K\in\mathcal{T}_h} \|u-\Pi_K^{k+2}(u)\|_{\sharp,K}^2.$$

Since $u - R_K(\widehat{u}_K) = (u-\mathcal{E}_K(u)) + R_K(\widehat{e}_K)$, the triangle inequality combined with Lemma 4.4 and the above bound proves (47). Furthermore, (48) results from (47) and the approximation properties of Π_K^{k+2} (using Lemma 2.7 and the multiplicative trace inequality (7)). Finally, (49) is proved similarly to (48), but this time invoking the fractional multiplicative trace inequality (10), in particular to bound $h_K^{\frac32}\|\partial_n\Delta(u-\Pi_K^2(u))\|_{\partial K} = h_K^{\frac32}\|\partial_n\Delta u\|_{\partial K}$. □

Remark 4.7 (Regularity gap) *The error estimates in Theorem 4.6 require $u \in H^{2+s}(\Omega)$ with $s > \frac12$. This global regularity requirement on the exact solution can be lowered to $s > 1$ by using the techniques developed in [29] and [28, Chap. 40&41] in the context of second-order elliptic PDEs. Indeed, the crucial point is to give a meaning to $\partial_n\Delta u$ on each mesh face, and this can be done by applying the tools from [29, 28] to the field $\nabla\Delta u$. Notice that the requirement $u \in H^{2+s}(\Omega)$ with $s > \frac12$ is, however, less stringent than the one resulting from achieving optimal decay rates as soon as $k \ge 1$ (see (48)).*

5 HHO method in arbitrary dimension

In this section, we adapt the material from the above two sections to devise and analyze an HHO method to approximate the biharmonic problem in arbitrary dimension $d \geq 2$. The main difference with the previous section is that the interpolation operator $J_{\partial K}^{k+1}$ is no longer available if $d \geq 3$. The idea in this section is to raise the degree of the face unknowns representing the solution trace to $(k+2)$, and to consider L^2-orthogonal projections to lead the analysis. Thus, letting $k \geq 0$ be the polynomial degree, the local HHO space considered in this section is such that for all $K \in \mathcal{T}_h$,

$$\widehat{V}_K^k := \mathbb{P}^{k+2}(K) \times \mathbb{P}^{k+2}(\mathcal{F}_{\partial K}) \times \mathbb{P}^k(\mathcal{F}_{\partial K}). \tag{50}$$

Remark 5.1 ($d = 3$) *In 3D, on tetrahedral meshes, one can also generalize the HHO method from the previous section by considering the canonical hybrid finite element of degree $(k+2)$ on the mesh faces.*

5.1 Reconstruction, stabilization, discrete problem, and stability

The local reconstruction operator is still defined by (18) (or, equivalently, (19)). Instead, the local stabilization bilinear form $S_{\partial K}$ has to be slightly modified and is now such that for all $(\widehat{v}_K, \widehat{w}_K) \in \widehat{V}_K^k \times \widehat{V}_K^k$,

$$S_{\partial K}(\widehat{v}_K, \widehat{w}_K) := h_K^{-3}\big(v_{\partial K} - v_K, w_{\partial K} - w_K\big)_{\partial K} + h_K^{-1}\big(\Pi_{\partial K}^k(\gamma_{\partial K} - \partial_n v_K), \Pi_{\partial K}^k(\chi_{\partial K} - \partial_n w_K)\big)_{\partial K}. \tag{51}$$

Notice that only L^2-orthogonal projections are considered. The local bilinear form a_K is defined on $\widehat{V}_K^k \times \widehat{V}_K^k$ as in (21).

The global HHO space is now defined as

$$\widehat{V}_h^k := \mathbb{P}^{k+2}(\mathcal{T}_h) \times \mathbb{P}^{k+2}(\mathcal{F}_h) \times \mathbb{P}^k(\mathcal{F}_h). \tag{52}$$

Focusing for simplicity on homogeneous boundary conditions, we consider the subspace $\widehat{V}_{h0}^k$ obtained by zeroing out all the components attached to the mesh boundary faces. The discrete HHO problem is as follows: Find $\widehat{u}_h \in \widehat{V}_{h0}^k$ such that

$$a_h(\widehat{u}_h, \widehat{w}_h) = \ell(w_{\mathcal{T}_h}), \qquad \forall w_h \in \widehat{V}_{h0}^k, \tag{53}$$

where a_h and ℓ are still defined as in (25). Moreover, as in the 2D setting, the discrete problem (53) is amenable to static condensation, whereby the cell unknowns are eliminated locally in every mesh cell, leading to a global problem where the only remaining unknowns are those attached to the mesh faces, i.e., those in $\mathbb{P}^{k+2}(\mathcal{F}_h) \times \mathbb{P}^k(\mathcal{F}_h)$.

Finally, it is readily seen that the local stability and boundedness property stated in Lemma 4.1 still holds true. Therefore, the discrete bilinear form a_h is coercive on $\widehat{V}_{h0}^k$, so that the discrete problem (53) is well-posed owing to the Lax–Milgram lemma.

Remark 5.2 (Comparison with [4]) *In the present HHO method, the global problem after static condensation features $(2k+4)$, $k \geq 0$, unknowns per mesh interface, whereas this number is $(4k+4)$, $k \geq 1$, for [4].*

Remark 5.3 (Boundary conditions) *In the non-homogeneous case, similarly to Remark 3.3, the value of the components of the HHO solution attached to the mesh boundary faces is assigned by means of the projections $\Pi_{\partial K}^{k+2}(g_D|_{\partial K})$ and $\Pi_{\partial K}^k(g_N|_{\partial K})$. It is also possible to enforce the boundary conditions $u = \partial_{nn} u = 0$ on $\partial\Omega$ by proceeding as in Remark 3.3.*

5.2 Polynomial approximation, consistency and error estimate

For all $K \in \mathcal{T}_h$, the local reduction operator $\widehat{\mathcal{I}}_K^k : H^2(K) \to \widehat{V}_K^k$ is now defined such that for all $v \in H^2(K)$,

$$\widehat{\mathcal{I}}_K^k(v) := (\Pi_K^{k+2}(v), \Pi_{\partial K}^{k+2}(v), \Pi_{\partial K}^k(\boldsymbol{n}_K \cdot \nabla v)) \in \widehat{V}_K^k. \tag{54}$$

We also define the operator $\widetilde{\mathcal{E}}_K := R_K \circ \widehat{\mathcal{I}}_K^k : H^2(K) \to \mathbb{P}^{k+2}(K)$. Although this operator is no longer the H^2-elliptic projection, we can show that it still enjoys the same approximation properties as those derived in Lemma 4.4. Recall that the $\|\cdot\|_{\sharp,K}$-norm is defined in (41).

Lemma 5.4 (Polynomial approximation) *The following holds true for all $K \in \mathcal{T}_h$ and all $v \in H^{2+s}(K)$ with $s > \frac{3}{2}$:*

$$\|v - \widetilde{\mathcal{E}}_K(v)\|_{\sharp,K} \le C\|v - \Pi_K^{k+2}(v)\|_{\sharp,K}. \tag{55}$$

Moreover, for all $K \in \mathcal{T}_h$ and all $v \in H^2(K)$, we have

$$S_{\partial K}(\widehat{\mathcal{I}}_K^k(v), \widehat{\mathcal{I}}_K^k(v))^{\frac{1}{2}} \le C\|v - \Pi_K^{k+2}(v)\|_{\sharp,K}. \tag{56}$$

Proof. (1) Using the definition (18) of R_K, the definition (54) of $\widehat{\mathcal{I}}_K^k$, and the orthogonality property of the L^2-projections Π_K^{k+2} and $\Pi_{\partial K}^{k+2}$, we infer that for all $w \in \mathbb{P}^{k+2}(K)$,

$$\begin{aligned}
(\nabla^2\widetilde{\mathcal{E}}_K(v), \nabla^2 w)_K &= (\nabla^2\Pi_K^{k+2}(v), \nabla^2 w)_K - (\Pi_{\partial K}^{k+2}(v) - \Pi_K^{k+2}(v), \partial_n\Delta w)_{\partial K} \\
&\quad + (\Pi_{\partial K}^{k}(\partial_n v) - \partial_n\Pi_K^{k+2}(v), \partial_{nn} w)_{\partial K} + (\partial_t(\Pi_{\partial K}^{k+2}(v) - \Pi_K^{k+2}(v)), \partial_{nt} w)_{\partial K} \\
&= (\nabla^2\Pi_K^{k+2}(v), \nabla^2 w)_K - (v - \Pi_K^{k+2}(v), \partial_n\Delta w)_{\partial K} \\
&\quad + (\partial_n(v - \Pi_K^{k+2}(v)), \partial_{nn} w)_{\partial K} + (\partial_t(\Pi_{\partial K}^{k+2}(v) - \Pi_K^{k+2}(v)), \partial_{nt} w)_{\partial K},
\end{aligned}$$

Taking $w := \widetilde{\mathcal{E}}_K(v) - \Pi_K^{k+2}(v)$, rearranging the terms, and invoking the Cauchy–Schwarz inequality together with the inverse inequalities (5), (6), (9) leads to

$$\begin{aligned}
&\|\nabla^2(\widetilde{\mathcal{E}}_K(v) - \Pi_K^{k+2}(v))\|_K \\
&\qquad \le C\big(h_K^{-\frac{3}{2}}\|v - \Pi_K^{k+2}(v)\|_{\partial K} + h_K^{-\frac{1}{2}}\|\partial_n(v - \Pi_K^{k+2}(v))\|_{\partial K} + h_K^{-\frac{3}{2}}\|\Pi_{\partial K}^{k+2}(v) - \Pi_K^{k+2}(v)\|_{\partial K}\big).
\end{aligned}$$

Concerning the rightmost term, we observe that $\Pi_{\partial K}^{k+2}(v) - \Pi_K^{k+2}(v) = \Pi_{\partial K}^{k+2}(v - \Pi_K^{k+2}(v))$, so that using the L^2-stability of $\Pi_{\partial K}^{k+2}$, we obtain

$$\|\nabla^2(\widetilde{\mathcal{E}}_K(v) - \Pi_K^{k+2}(v))\|_K \le C\big(h_K^{-\frac{3}{2}}\|v - \Pi_K^{k+2}(v)\|_{\partial K} + h_K^{-\frac{1}{2}}\|\partial_n(v - \Pi_K^{k+2}(v))\|_{\partial K}\big).$$

The trace inequality (12) then shows that

$$\|\nabla^2(\widetilde{\mathcal{E}}_K(v) - \Pi_K^{k+2}(v))\|_K \le C\|\nabla^2(v - \Pi_K^{k+2}(v))\|_K.$$

The proof of (55) can now be completed by invoking the triangle inequality.
(2) Let us now prove (56). We have

$$S_{\partial K}(\widehat{\mathcal{I}}_K^k(v), \widehat{\mathcal{I}}_K^k(v))^{\frac{1}{2}} \le h_K^{-\frac{3}{2}}\|\Pi_{\partial K}^{k+2}(v) - \Pi_K^{k+2}(v)\|_{\partial K} + h_K^{-\frac{1}{2}}\|\Pi_{\partial K}^{k}(\partial_n v - \partial_n\Pi_K^{k+2}(v))\|_{\partial K},$$

where we used that $\Pi_{\partial K}^k \circ \Pi_{\partial K}^k = \Pi_{\partial K}^k$ for the second term on the right-hand side. To bound the first term on the right-hand side, we invoke the same arguments as in the first step of this proof leading to

$$h_K^{-\frac{3}{2}}\|\Pi_{\partial K}^{k+2}(v) - \Pi_K^{k+2}(v)\|_{\partial K} \le C\|\nabla^2(v - \Pi_K^{k+2}(v))\|_K.$$

Furthermore, the second term has already been bounded in the proof of Lemma 4.3. This completes the proof. □

The global reduction operator $\widehat{\mathcal{I}}_h^k : H^2(\Omega) \to \widehat{V}_h^k$ is defined such that for all $v \in H^2(\Omega)$,

$$\widehat{\mathcal{I}}_h^k(v) := \big((\Pi_K^{k+2}(v))_{K\in\mathcal{T}_h}, (\Pi_F^{k+2}(v))_{F\in\mathcal{F}_h}, (\Pi_F^k(\boldsymbol{n}_F\cdot\nabla v))_{F\in\mathcal{F}_h}\big) \in \widehat{V}_h^k, \tag{57}$$

so that the local components of $\widehat{\mathcal{I}}_h^k(v)$ are $\widehat{\mathcal{I}}_K^k(v|_K)$ for all $K \in \mathcal{T}_h$. The consistency error $\delta_h \in (\widehat{V}_{h0}^k)'$ can now be defined as in (44) and it can be bounded as in Lemma 4.5. Finally, the error estimate and its proof are the same as those from Theorem 4.6 (and are not repeated for brevity).

6 HHO method with Nitsche's boundary penalty

In this section, we combine the HHO methods devised in the previous sections with Nitsche's boundary-penalty technique to enforce the boundary conditions in a weak manner. For brevity, we only discuss the HHO method presented in Section 3, but the following developments can be readily applied to the HHO method from Section 5. To allow for a bit more generality, we detail here the case of non-homogeneous boundary conditions. Thus, the model problem is as follows:

$$\Delta^2 u = f \text{ in } \Omega, \qquad u = g_D,\ \partial_n u = g_N \text{ in } \partial\Omega, \tag{58}$$

where the assumptions on the boundary data g_D and g_N are given in Remark 2.1. We set $\boldsymbol{G} := (\nabla u)|_{\partial\Omega}$ and notice that $\boldsymbol{G}$ is explicitly known in terms of the boundary data g_D and g_N since $\boldsymbol{G} = g_N\boldsymbol{n} + (\partial_t g_D)\boldsymbol{t}$.

Hinging on the ideas from [8, 7] for second-order elliptic PDEs, the HHO-Nitsche (HHO-N) method devised in this section does not place any discrete unknown on the mesh boundary faces, but only in the mesh cells and the mesh interfaces. Thus, for every mesh cell $K \in \mathcal{T}_h$, we define the subsets

$$\partial K^{\mathrm{i}} := \overline{\partial K \cap \Omega}, \qquad \partial K^{\mathrm{b}} := \partial K \cap \partial\Omega, \tag{59}$$

as well as $\mathcal{F}_{\partial K^{\mathrm{i}}} := \mathcal{F}_{\partial K} \cap \mathcal{F}_h^{\mathrm{i}}$ and $\mathcal{F}_{\partial K^{\mathrm{b}}} := \mathcal{F}_{\partial K} \cap \mathcal{F}_h^{\mathrm{b}}$. The mesh cells having at least one boundary face are collected in the subset $\mathcal{T}_h^{\mathrm{b}} := \{K \in \mathcal{T}_h \mid \mathcal{F}_{\partial K^{\mathrm{b}}} \neq \emptyset\}$, and we set $\mathcal{T}_h^{\mathrm{i}} := \mathcal{T}_h \setminus \mathcal{T}_h^{\mathrm{b}}$.

Letting $k \geq 0$ be the polynomial degree, the local HHO-N space is such that for all $K \in \mathcal{T}_h$,

$$\widehat{V}_K^k := \mathbb{P}^{k+2}(K) \times \mathbb{P}^{k+1}(\mathcal{F}_{\partial K^{\mathrm{i}}}) \times \mathbb{P}^k(\mathcal{F}_{\partial K^{\mathrm{i}}}), \tag{60}$$

and the corresponding global HHO-N space is now defined as

$$\widehat{V}_h^k := \mathbb{P}^{k+2}(\mathcal{T}_h) \times \mathbb{P}^{k+1}(\mathcal{F}_h^{\mathrm{i}}) \times \mathbb{P}^k(\mathcal{F}_h^{\mathrm{i}}). \tag{61}$$

6.1 Reconstruction, stabilization, discrete problem, and stability

The definition of the local reconstruction operator is slightly modified with respect to (18). Indeed, $R_K^{\mathrm{i}} : \widehat{V}_K^k \to \mathbb{P}^{k+2}(K)$ is now such that for all $\widehat{v}_K \in \widehat{V}_K^k$,

$$\begin{aligned}(\nabla^2 R_K^{\mathrm{i}}(\widehat{v}_K), \nabla^2 w)_K = (\nabla^2 v_K, \nabla^2 w)_K + (v_K - v_{\partial K}, \partial_n\Delta w)_{\partial K^{\mathrm{i}}} - (\partial_n v_K - \gamma_{\partial K}, \partial_{nn} w)_{\partial K^{\mathrm{i}}} \\ - (\partial_t(v_K - v_{\partial K}), \partial_{nt} w)_{\partial K^{\mathrm{i}}} + (v_K, \partial_n\Delta w)_{\partial K^{\mathrm{b}}} - (\nabla v_K, \nabla\partial_n w)_{\partial K^{\mathrm{b}}},\end{aligned} \tag{62}$$

for all $w \in \mathbb{P}^{k+2}(K)^\perp$ together with the condition $(R_K^{\mathrm{i}}(\widehat{v}_K), \xi)_K = (v_K, \xi)_K$ for all $\xi \in \mathbb{P}^1(K)$. Equivalently, owing to the integration by parts formula (3), we have

$$(\nabla^2 R_K^{\mathrm{i}}(\widehat{v}_K), \nabla^2 w)_K = (v_K, \Delta^2 w)_K - (v_{\partial K}, \partial_n\Delta w)_{\partial K^{\mathrm{i}}} + (\gamma_{\partial K}, \partial_{nn} w)_{\partial K^{\mathrm{i}}} + (\partial_t v_{\partial K}, \partial_{nt} w)_{\partial K^{\mathrm{i}}}. \tag{63}$$

Dropping the integral over ∂K^{b} for the three rightmost terms in (63) is, loosely speaking, a consistent operation in the case of homogeneous boundary conditions. In the general case, we need to lift the boundary data in every mesh cell $K \in \mathcal{T}_h^{\mathrm{b}}$ by means of the lifting operator $\mathcal{L}_K : H^2(K) \to \mathbb{P}^{k+2}(K)$ such that for all $v \in H^2(K)$,

$$(\nabla^2 \mathcal{L}_K(v), \nabla^2 w)_K = -(v, \partial_n\Delta w)_{\partial K^{\mathrm{b}}} + (\nabla v, \nabla\partial_n w)_{\partial K^{\mathrm{b}}}, \tag{64}$$

for all $w \in \mathbb{P}^{k+2}(K)^\perp$, together with the condition $(\mathcal{L}_K(v), \xi)_K = 0$ for all $\xi \in \mathbb{P}^1(K)$. Notice that $\mathcal{L}_K(u|_K)$ is fully computable from the boundary data g_D and g_N. For convenience, we set $\mathcal{L}_K(v) := 0$ for all $K \in \mathcal{T}_h^{\mathrm{i}}$.

The local stabilization bilinear form $S_{\partial K}$ is also slightly modified and is now such that for all $(\widehat{v}_K, \widehat{w}_K) \in \widehat{V}_K^k \times \widehat{V}_K^k$, we have $S_{\partial K}(\widehat{v}_K, \widehat{w}_K) := S_{\partial K}^{\mathrm{i}}(\widehat{v}_K, \widehat{w}_K) + S_{\partial K}^{\mathrm{b}}(v_K, w_K)$ with

$$\begin{aligned}S_{\partial K}^{\mathrm{i}}(\widehat{v}_K, \widehat{w}_K) := h_K^{-3}\big(J_{\partial K}^{k+1}(v_{\partial K} - v_K), J_{\partial K}^{k+1}(w_{\partial K} - w_K)\big)_{\partial K^{\mathrm{i}}} \\ + h_K^{-1}\big(\Pi_{\partial K}^k(\gamma_{\partial K} - \partial_n v_K), \Pi_{\partial K}^k(\chi_{\partial K} - \partial_n w_K)\big)_{\partial K^{\mathrm{i}}},\end{aligned} \tag{65}$$

$$S_{\partial K}^{\mathrm{b}}(v_K, w_K) := h_K^{-3}\big(v_K, w_K\big)_{\partial K^{\mathrm{b}}} + h_K^{-1}\big(\nabla v_K, \nabla w_K\big)_{\partial K^{\mathrm{b}}}, \tag{66}$$

where $S_{\partial K}^{\mathrm{b}}$ represents the boundary-penalty contribution and acts only on the cell components. We emphasize that $S_{\partial K}^{\mathrm{b}}$ does not need to be scaled by a weighting coefficient to be taken large enough. Finally, the local bilinear form a_K is defined on $\widehat{V}_K^k \times \widehat{V}_K^k$ as in (21).

The discrete HHO-N problem is as follows: Find $\widehat{u}_h \in \widehat{V}_h^k$ such that

$$a_h(\widehat{u}_h, \widehat{w}_h) = \ell_h(\widehat{w}_h), \qquad \forall \widehat{w}_h \in \widehat{V}_h^k, \tag{67}$$

where a_h is still assembled cellwise as in (25) yielding

$$a_h(\widehat{v}_h, \widehat{w}_h) := \sum_{K\in\mathcal{T}_h} (\nabla^2 R_K^{\mathrm{i}}(\widehat{v}_K), \nabla^2 R_K^{\mathrm{i}}(\widehat{w}_K))_K + \sum_{K\in\mathcal{T}_h} S_{\partial K}^{\mathrm{i}}(\widehat{v}_K, \widehat{w}_K) + \sum_{K\in\mathcal{T}_h^{\mathrm{b}}} S_{\partial K}^{\mathrm{b}}(v_K, w_K), \tag{68}$$

whereas the linear form ℓ_h now acts as follows:

$$\begin{aligned}\ell_h(\widehat{w}_h) := \sum_{K\in\mathcal{T}_h} (f, w_K)_K + \sum_{K\in\mathcal{T}_h^{\mathrm{b}}} \Big\{ & h_K^{-3}(g_D, w_K)_{\partial K^{\mathrm{b}}} + h_K^{-1}(\boldsymbol{G}, \nabla w_K)_{\partial K^{\mathrm{b}}} \\ & + \big(g_D, \partial_n \Delta R_K^{\mathrm{i}}(\widehat{w}_K)\big)_{\partial K^{\mathrm{b}}} - \big(\boldsymbol{G}, \nabla \partial_n R_K^{\mathrm{i}}(\widehat{w}_K)\big)_{\partial K^{\mathrm{b}}} \Big\}.\end{aligned} \tag{69}$$

Notice that

$$\ell_h(\widehat{w}_h) = \sum_{K\in\mathcal{T}_h} (f, w_K)_K + \sum_{K\in\mathcal{T}_h^{\mathrm{b}}} \Big\{ S_{\partial K}^{\mathrm{b}}(u|_K, w_K) - (\nabla^2 \mathcal{L}_K(u|_K), \nabla^2 R_K^{\mathrm{i}}(\widehat{w}_K))_K \Big\}. \tag{70}$$

Notice also that $\ell_h(\widehat{w}_h) = \sum_{K\in\mathcal{T}_h} (f, w_K)_K = (f, w_{\mathcal{T}_h})_\Omega$ if the boundary conditions are homogeneous (so that only the cell component of $\widehat{w}_h$ is needed to assemble ℓ_h). As in the previous sections, the discrete problem (67) is amenable to static condensation, whereby all the cell unknowns are eliminated locally in every mesh cell, leading to a global problem where the only remaining unknowns are those attached to the mesh interfaces.

It is easy to see that the local stability and boundedness property stated in Lemma 4.1 still holds true in the updated H^2-seminorm

$$|\widehat{v}_K|_{\widehat{V}_K^k}^2 := \|\nabla^2 v_K\|_K^2 + h_K^{-3}\|v_{\partial K} - v_K\|_{\partial K^{\mathrm{i}}}^2 + h_K^{-1}\|\gamma_{\partial K} - \partial_n v_K\|_{\partial K^{\mathrm{i}}}^2 + S_{\partial K}^{\mathrm{b}}(v_K, v_K), \tag{71}$$

recalling that $S_{\partial K}^{\mathrm{b}}(v_K, v_K) = h_K^{-3}\|v_K\|_{\partial K^{\mathrm{b}}}^2 + h_K^{-1}\|\nabla v_K\|_{\partial K^{\mathrm{b}}}^2$. Since $\|\widehat{v}_h\|_{\widehat{V}_h^k}^2 := \sum_{K\in\mathcal{T}_h} |\widehat{v}_K|_{\widehat{V}_K^k}^2$ defines a norm on the global HHO space $\widehat{V}_h^k$ defined in (61), the discrete bilinear form a_h is coercive on $\widehat{V}_h^k$, and the discrete problem (67) is well-posed owing to the Lax–Milgram lemma.

6.2 Polynomial approximation, consistency and error estimate

For all $K \in \mathcal{T}_h$, we define the local reduction operator $\widehat{\mathcal{I}}_K^k : H^2(K) \to \widehat{V}_K^k$ such that for all $v \in H^2(K)$,

$$\widehat{\mathcal{I}}_K^k(v) := \big(\Pi_K^{k+2}(v), J_{\partial K^{\mathrm{i}}}^{k+1}(v), \Pi_{\partial K^{\mathrm{i}}}^k(\boldsymbol{n}_K\cdot\nabla v)\big) \in \widehat{V}_K^k, \tag{72}$$

with obvious notation regarding the operators $J_{\partial K^{\mathrm{i}}}^{k+1}$ and $\Pi_{\partial K^{\mathrm{i}}}^k$. Let us set

$$\mathcal{E}_K^{\mathrm{i}} := R_K^{\mathrm{i}} \circ \widehat{\mathcal{I}}_K^k : H^2(K) \to \mathbb{P}^{k+2}(K). \tag{73}$$

A straightforward verification (omitted for brevity) shows that the operator $\mathcal{E}_K := \mathcal{E}_K^{\mathrm{i}} + \mathcal{L}_K : H^2(K) \to \mathbb{P}^{k+2}(K)$ coincides indeed with the H^2-elliptic projection defined in (38). Therefore, owing to Lemma 4.4, there is C such that for all $K \in \mathcal{T}_h$ and all $v \in H^{2+s}(K)$, $s > \frac{3}{2}$,

$$\|v - (\mathcal{E}_K^{\mathrm{i}}(v) + \mathcal{L}_K(v))\|_{\sharp,K} \le C\|v - \Pi_K^{k+2}(v)\|_{\sharp,K}, \tag{74}$$

where the $\|\cdot\|_{\sharp,K}$-norm is defined in (41). Moreover, by restricting the arguments to the mesh interfaces in the proof of Lemma 4.3, we infer that there is C such that for all $K \in \mathcal{T}_h$ and all $v \in H^2(K)$,

$$S_{\partial K}^{\mathrm{i}}(\widehat{\mathcal{I}}_K^k(v), \widehat{\mathcal{I}}_K^k(v))^{\frac{1}{2}} \le C\|\nabla^2(v - \Pi_K^{k+2}(v))\|_K. \tag{75}$$

The global reduction operator $\widehat{\mathcal{I}}_h^k : H^2(\Omega) \to \widehat{V}_h^k$ is defined such that for all $v \in H^2(\Omega)$,

$$\widehat{\mathcal{I}}_h^k(v) := \big((\Pi_K^{k+2}(v))_{K\in\mathcal{T}_h}, (J_F^{k+1}(v))_{F\in\mathcal{F}_h^{\mathrm{i}}}, (\Pi_F^k(\boldsymbol{n}_F\cdot\nabla v))_{F\in\mathcal{F}_h^{\mathrm{i}}}\big) \in \widehat{V}_h^k, \tag{76}$$

recalling that v and ∇v are single-valued on every $F \in \mathcal{F}_h^{\mathrm{i}}$ for all $v \in H^2(\Omega)$. As above, the local components of $\widehat{\mathcal{I}}_h^k(v)$ attached to K and its faces in $\mathcal{F}_{\partial K^{\mathrm{i}}}$ are $\widehat{\mathcal{I}}_K^k(v|_K)$ for all $K \in \mathcal{T}_h$. We define the consistency error $\delta_h \in (\widehat{V}_h^k)'$ such that $\langle \delta_h, \widehat{w}_h\rangle := \ell(w_{\mathcal{T}_h}) - a_h(\widehat{\mathcal{I}}_h^k(u), \widehat{w}_h)$, for all $\widehat{w}_h \in \widehat{V}_h^k$, where $\langle\cdot,\cdot\rangle$ now denotes the duality pairing between $(\widehat{V}_h^k)'$ and $\widehat{V}_h^k$.

Lemma 6.1 (Consistency) *Assume that $u \in H^{2+s}(\Omega)$ with $s > \frac{3}{2}$. The following holds true:*

$$\|\delta_h\|_{(\widehat{V}_h^k)'} := \sup_{\widehat{w}_h\in\widehat{V}_h^k} \frac{|\langle\delta_h,\widehat{w}_h\rangle|}{\|\widehat{w}_h\|_{\widehat{V}_h^k}} \le C\left(\sum_{K\in\mathcal{T}_h} \|u - \Pi_K^{k+2}(u)\|_{\sharp,K}^2\right)^{\frac12}. \tag{77}$$

Proof. The proof is similar to that of Lemma 4.5, so we only sketch it. Let $\widehat{w}_h \in \widehat{V}_h^k$ having local components $(w_K, w_{\partial K}, \chi_{\partial K})$ for all $K \in \mathcal{T}_h$. On the one hand, we have

$$\begin{aligned}
&\ell_h(\widehat{w}_h) + \sum_{K\in\mathcal{T}_h^{\mathrm{b}}} (\nabla^2\mathcal{L}_K(u|_K), \nabla^2(R_K^{\mathrm{i}}(\widehat{w}_K)))_K\\
&= \sum_{K\in\mathcal{T}_h}\Big\{(\nabla^2 u, \nabla^2 w_K)_K + (\partial_n\Delta u, w_K)_{\partial K^{\mathrm{b}}} - (\nabla\partial_n u, \nabla w_K)_{\partial K^{\mathrm{b}}}\\
&\quad + (\partial_n\Delta u, w_K - w_{\partial K})_{\partial K^{\mathrm{i}}} - (\partial_{nn}u, \partial_n w_K - \chi_{\partial K})_{\partial K^{\mathrm{i}}} - (\partial_{nt}u, \partial_t(w_K - w_{\partial K}))_{\partial K^{\mathrm{i}}}\Big\}\\
&\quad + \sum_{K\in\mathcal{T}_h^{\mathrm{b}}}\Big\{h_K^{-3}(u, w_K)_{\partial K^{\mathrm{b}}} + h_K^{-1}(\nabla u, \nabla w_K)_{\partial K^{\mathrm{b}}}\Big\}.
\end{aligned}$$

On the other hand, recalling that $\mathcal{E}_K = \mathcal{E}_K^{\mathrm{i}} + \mathcal{L}_K$, we have

$$\begin{aligned}
&a_h(\widehat{\mathcal{I}}_h^k(u), \widehat{w}_h) + \sum_{K\in\mathcal{T}_h^{\mathrm{b}}} (\nabla^2\mathcal{L}_K(u|_K), \nabla^2(R_K^{\mathrm{i}}(\widehat{w}_K)))_K\\
&= \sum_{K\in\mathcal{T}_h}\Big\{(\nabla^2\mathcal{E}_K(u), \nabla^2 R_K^{\mathrm{i}}(\widehat{w}_K))_K + S_{\partial K}^{\mathrm{i}}(\widehat{\mathcal{I}}_K^k(u), \widehat{w}_K)\Big\} + \sum_{K\in\mathcal{T}_h^{\mathrm{b}}} S_{\partial K}^{\mathrm{b}}(\Pi_K^{k+2}(u), w_K),
\end{aligned}$$

so that we have

$$\begin{aligned}
&a_h(\widehat{\mathcal{I}}_h^k(u), \widehat{w}_h) + \sum_{K\in\mathcal{T}_h^{\mathrm{b}}} (\nabla^2\mathcal{L}_K(u|_K), \nabla^2(R_K^{\mathrm{i}}(\widehat{w}_K)))_K\\
&= \sum_{K\in\mathcal{T}_h}\Big\{(\nabla^2\mathcal{E}_K(u), \nabla^2 w_K)_K + (\partial_n\Delta\mathcal{E}_K(u), w_K)_{\partial K^{\mathrm{b}}} - (\nabla\partial_n\mathcal{E}_K(u), \nabla w_K)_{\partial K^{\mathrm{b}}}\\
&\quad + (\partial_n\Delta\mathcal{E}_K(u), w_K - w_{\partial K})_{\partial K^{\mathrm{i}}} - (\partial_{nn}\mathcal{E}_K(u), \partial_n w_K - \chi_{\partial K})_{\partial K^{\mathrm{i}}} - (\partial_{nt}\mathcal{E}_K(u), \partial_t(w_K - w_{\partial K}))_{\partial K^{\mathrm{i}}}\\
&\quad + S_{\partial K}^{\mathrm{i}}(\widehat{\mathcal{I}}_K^k(u), \widehat{w}_K)\Big\} + \sum_{K\in\mathcal{T}_h^{\mathrm{b}}}\Big\{h_K^{-3}(\Pi_K^{k+2}(u), w_K)_{\partial K^{\mathrm{b}}} + h_K^{-1}(\nabla\Pi_K^{k+2}(u), \nabla w_K)_{\partial K^{\mathrm{b}}}\Big\}.
\end{aligned}$$

Defining the function η cellwise as $\eta|_K := u|_K - \mathcal{E}_K(u|_K)$ for all $K \in \mathcal{T}_h$, we infer that

$$\begin{aligned}
\langle\delta_h, \widehat{w}_h\rangle &= \sum_{K\in\mathcal{T}_h}\Big\{(\nabla^2\eta, \nabla^2 w_K)_K + (\partial_n\Delta\eta, w_K)_{\partial K^{\mathrm{b}}} - (\nabla\partial_n\eta, \nabla w_K)_{\partial K^{\mathrm{b}}}\\
&\quad + (\partial_n\Delta\eta, w_K - w_{\partial K})_{\partial K^{\mathrm{i}}} - (\partial_{nn}\eta, \partial_n w_K - \chi_{\partial K})_{\partial K^{\mathrm{i}}} - (\partial_{nt}\eta, \partial_t(w_K - w_{\partial K}))_{\partial K^{\mathrm{i}}} - S_{\partial K}^{\mathrm{i}}(\widehat{\mathcal{I}}_K^k(u), \widehat{w}_K)\Big\}\\
&\quad + \sum_{K\in\mathcal{T}_h^{\mathrm{b}}}\Big\{h_K^{-3}(u - \Pi_K^{k+2}(u), w_K)_{\partial K^{\mathrm{b}}} + h_K^{-1}(\nabla(u - \Pi_K^{k+2}(u)), \nabla w_K)_{\partial K^{\mathrm{b}}}\Big\}.
\end{aligned}$$

All the terms on the right-hand side can now be bounded by means of the Cauchy–Schwarz inequality. For the first, fourth, fifth, and sixth terms, we use (74), for the seventh term (involving $S_{\partial K}^{\mathrm{i}}$), we use (75), and for the eighth and ninth terms, we invoke the trace inequality (12).

□

We are now ready to establish our main error estimate.

Theorem 6.2 (H^2-error estimate) *Assume that $u \in H^{2+s}(\Omega)$ with $s > \frac{3}{2}$. The following holds true:*

$$\sum_{K\in\mathcal{T}_h} \|\nabla^2(u - R_K^{\rm i}(\widehat{u}_K) - \mathcal{L}_K(u))\|_K^2 \le C \sum_{K\in\mathcal{T}_h} \|u - \Pi_K^{k+2}(u)\|_{\sharp,K}^2. \tag{78}$$

Consequently, if $k \ge 1$, assuming $u|_K \in H^{k+3}(K)$ for all $K \in \mathcal{T}_h$, we have

$$\sum_{K\in\mathcal{T}_h} \|\nabla^2(u - R_K^{\rm i}(\widehat{u}_K) - \mathcal{L}_K(u))\|_K^2 \le C \sum_{K\in\mathcal{T}_h} \left(h_K^{k+1}|u|_{H^{k+3}(K)}\right)^2, \tag{79}$$

and if $k = 0$, letting $\sigma := \min(s-1, 1) \in (\frac{1}{2}, 1]$, we have

$$\sum_{K\in\mathcal{T}_h} \|\nabla^2(u - R_K^{\rm i}(\widehat{u}_K) - \mathcal{L}_K(u))\|_K^2 \le C \sum_{K\in\mathcal{T}_h} \left(h_K(|u|_{H^3(K)} + h_K^\sigma |u|_{H^{3+\sigma}(K)})\right)^2. \tag{80}$$

Proof. As in the proof of Theorem 4.6, one shows that

$$\sum_{K\in\mathcal{T}_h} \|\nabla^2 R_K^{\rm i}(\widehat{e}_K)\|_K^2 \le C \sum_{K\in\mathcal{T}_h} \|u - \Pi_K^{k+2}(u)\|_{\sharp,K}^2,$$

where $\widehat{e}_h := \widehat{\mathcal{I}}_h^k(u) - \widehat{u}_h \in \widehat{V}_h^k$ is the discrete error. Since $u - R_K^{\rm i}(\widehat{u}_K) - \mathcal{L}_K(u) = (u - \mathcal{E}_K^{\rm i}(u) - \mathcal{L}_K(u)) + R_K^{\rm i}(\widehat{e}_K)$ for all $K \in \mathcal{T}_h$, the triangle inequality combined with (74) and the above bound on the discrete error proves (47). Finally, (79) and (80) are established by invoking the same arguments as above. □

7 Numerical examples

In this section, we present numerical examples to illustrate the theoretical results on the present HHO methods and also to compare their numerical performance with respect to other methods from the literature.

7.1 Convergence rates and computational performance of HHO methods

We select f on $\Omega := (0,1)^2$ so that the exact solution to (1) is $u(x,y) = \sin(\pi x)^2 \sin(\pi y)^2$ with homogeneous boundary conditions. We consider the two HHO methods analyzed above. For clarity, we term "HHO(A)" the method introduced in Section 3 with discrete unknowns in $\mathbb{P}^{k+2}(\mathcal{T}_h) \times \mathbb{P}^{k+1}(\mathcal{F}_h^{\rm i}) \times \mathbb{P}^k(\mathcal{F}_h^{\rm i})$ and "HHO(B)" the method introduced in Section 5 with discrete unknowns in $\mathbb{P}^{k+2}(\mathcal{T}_h) \times \mathbb{P}^{k+2}(\mathcal{F}_h^{\rm i}) \times \mathbb{P}^k(\mathcal{F}_h^{\rm i})$. Additionally, we consider the method termed "HHO(C)" mentioned in Remark 3.2 where the discrete unknowns are in $\mathbb{P}^{k+1}(\mathcal{T}_h) \times \mathbb{P}^{k+1}(\mathcal{F}_h^{\rm i}) \times \mathbb{P}^k(\mathcal{F}_h^{\rm i})$. We employ polynomial degrees $k \in \{0, \dots, 5\}$. Since we consider various polynomial degrees, and despite an *hp*-analysis falls beyond the present scope, we implement the stabilization terms in (20), (51), and (26) with h_K^{-1} replaced by $(k+1)^2 h_K^{-1}$ for all $K \in \mathcal{T}_h$. All the computations were run with Matlab R2018a on the NEF platform at INRIA Sophia Antipolis Méditerranée using 12 cores, and all the linear systems after static condensation are solved using the `backslash` function. The algorithm for solving the symmetric positive definite linear systems is the Cholesky factorization.

Let us first verify the convergence rates obtained with the HHO(A) method with $k \in \{0, 1, 2, 3\}$. We consider a sequence of successively refined rectangular meshes and a sequence of successively refined polygonal (Voronoi-like) meshes (generated through the PolyMesher Matlab library [43]). Two examples of polygonal meshes are shown in Figure 1 (in general, the cells do not contain more than 8 edges). We measure relative errors in the (broken) H^2-seminorm and in the L^2-norm, both quantities being evaluated using the reconstruction of the HHO solution cellwise. The errors are reported in Figure 2 as a function of $\text{DoFs}^{1/2}$, where DoFs denotes the total number of globally coupled discrete unknowns (that is, the face unknowns). We observe that the H^2-error converges at the optimal rate $O(h^{k+1})$, as predicted in Theorem 4.6. The L^2-error converges at the optimal rate $O(h^{k+3})$, except for $k = 0$ where

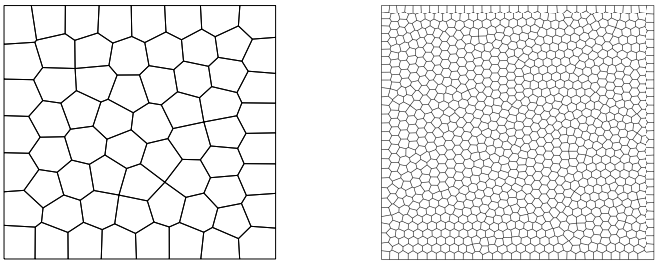

Figure 1: Two examples of polygonal (Voronoi-like) meshes with 64 (left) and 1,024 polygons

.

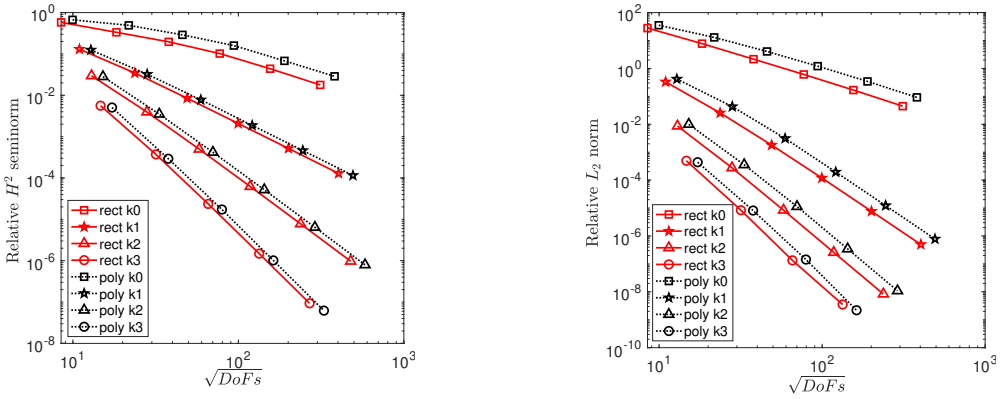

Figure 2: Convergence of HHO(A) method in H^2- and L^2-(semi)norms on polygonal and rectangular meshes.

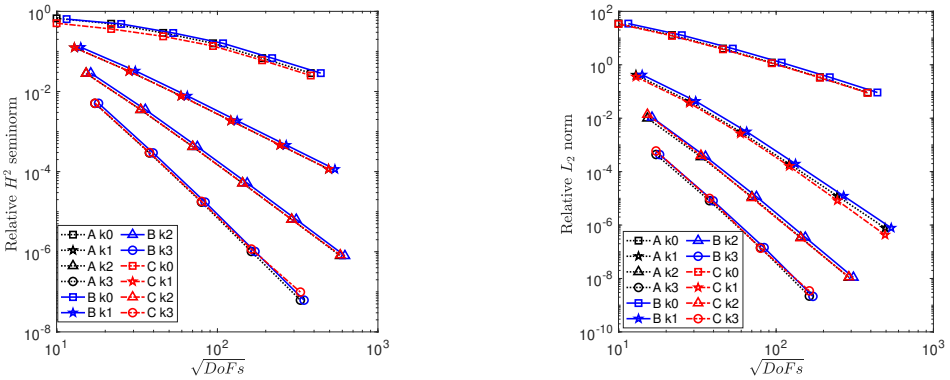

Figure 3: Convergence of HHO(A,B,C) methods in H^2- and L^2-(semi)norms on polygonal meshes.

the rate is only $O(h^2)$; all these rates are consistent with what can be expected from a duality argument (not detailed herein for brevity; see [4, 38] for examples of this argument for HHO and WG methods).

Let us now compare the three HHO(A,B,C) methods. The same relative errors as in Figure 2 are reported in Figure 3. The results show that the three HHO methods converge with the same rates, and that the accuracy reached on a given mesh with a given polynomial degree is quite close for the three methods. We mention that the three methods are sensitive to conditioning issues that arise for high polynomial degree when the error is already quite low (typically below 10^{-8} in the H^2-seminorm), and the HHO(C) method is somewhat more sensitive. It is instructive to have a closer look at how the computational costs related to the assembling of the system matrix are spent between the tasks of reconstruction, stabilization, and static condensation. The results are reported in Figure 4 on a polygonal mesh with 16,384 cells (and 49,014 edges) and polynomial degrees $k \in \{0, \ldots, 5\}$. Quite importantly, the local reconstruction operator is computed based on equation (19). Indeed, using (18) instead results

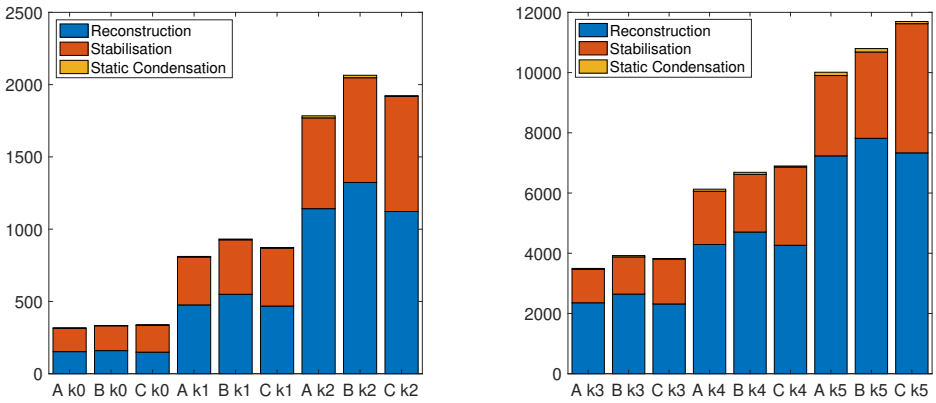

Figure 4: Comparison of computational times (in seconds) spent in reconstruction, stabilization, and static condensation for the three HHO(A,B,C) methods on a polygonal mesh with 16,384 cells and polynomial degrees $k \in \{0, \dots, 5\}$.

in a more intricate assembling of the right-hand side, increasing by a factor ranging from 2.5 (for $k = 0$) to 3.5 (for $k = 5$) the time spent in reconstruction. Figure 4 shows that the time spent on static condensation is always marginal. Moreover, we can see that the somewhat more elaborate design of the stabilization in the HHO(C) method is reflected by a somewhat larger computational cost than for the HHO(A,B) methods. The (perhaps a bit unexpected) consequence is that the HHO(A,B) methods require altogether less assembly time than the HHO(C) method although their number of discrete unknowns is larger. Finally, we notice that the reconstruction time is always larger than the stabilization time, and this trend gets more pronounced for larger k. To sum up, the most computationally effective method based on these results is HHO(A). In what follows, we only consider this method and simply call it "HHO" method.

7.2 Comparison with DG, C^0-IPDG, and FEM

In this section, we compare the computational performance of HHO with the fully nonconforming dG method on polygonal and simpler meshes, and with the C^0-IPDG, Morley, and HCT methods on triangular meshes.

HHO, triangular mesh				dG, triangular mesh			
order	# DoFs	assembling	solving	order	# DoFs	assembling	solving
$k = 0$	146,688	275.5	7.0	$\ell = 2$	196,608	472.0	16.0
$k = 1$	244,480	882.0	18.3	$\ell = 3$	327,680	1300.9	41.1
$k = 2$	342,272	2076.3	33.2	$\ell = 4$	491,520	2965.4	96.0
$k = 3$	440,064	4062.0	53.0	$\ell = 5$	688,128	5940.6	195.1

HHO, polygonal mesh				dG, polygonal mesh			
order	# DoFs	assembling	solving	order	# DoFs	assembling	solving
$k = 0$	145,554	251.1	17.3	$\ell = 2$	98,304	420.5	12.7
$k = 1$	242,590	770.2	44.7	$\ell = 3$	163,840	1160.9	33.1
$k = 2$	339,626	1784.3	86.9	$\ell = 4$	245,760	2647.3	78.4
$k = 3$	436,662	3496.7	149.9	$\ell = 5$	344,064	5304.7	155.8

Table 2: Comparison of total DoFs, assembling time, and solving time for the HHO and dG methods. The polynomial degree is chosen so that both methods deliver the same decay rates on the H^2-error. Upper table: triangular mesh composed of 32,768 cells; lower table: polygonal mesh composed of 16,384 cells.

Let us consider first the dG method. To put HHO and dG on a fair comparison basis, we compare

the HHO method with face polynomial degree $k \geq 0$ to the dG method with cell polynomial degree $\ell = k + 2$, so that both methods deliver the same decay rates on the H^2-error. A comparison of total DoFs, assembling time (including static condensation if applicable), and solving time for both methods is provided in Table 2. We consider a triangular mesh and a polygonal mesh (with 32,768 and 16,384 cells, respectively). The first observation is that HHO always leads to less DoFs, and to smaller times spent on assembling. The main reason is that the HHO DoFs are attached to the mesh faces rather than the mesh cells. Although there are more faces than cells in a given mesh (the more so as the cells are polygons with many faces), the polynomial spaces in cells are richer than those on faces. Moreover, the degree of the cell polynomials in the dG method is larger than the degree of the face polynomials in the HHO method ($(k+2)$ vs. $\{k, k+1\}$). Another reason for the lower assembling times with HHO is that the evaluation of numerical fluxes in dG methods actually leads to a more expensive evaluation of face-related quantities. The conclusions are, however, slightly different if one considers the solving time (since the assembling stage can be fully parallelized, the solving time becomes dominant in highly parallel architectures). The results in Table 2 show that on triangular meshes (where cells have a moderate number of faces), the solving time for HHO is always smaller than that for dG. Instead, on polygonal (Voronoi-like) meshes, the solving time for dG is smaller for low polynomial degrees (up to 2), whereas the solving time for HHO becomes again smaller for higher polynomial degrees. The observation on polygonal meshes and low polynomial degrees indicates that although the stencil of HHO methods is quite compact, it is still less compact than that of dG methods. In particular, all the discrete unknowns attached to the faces sharing a given mesh cell are coupled. Figure 5 provides a more thorough viewpoint on the above results by highlighting the relative efficiency of both methods measured as the time needed to reach a certain error threshold in the H^2-seminorm. The time is either the assembling time (which is more representative of a serial implementation) or the solving time (which is more representative of a parallel implementation). We can see that on triangular and rectangular meshes, for all polynomial orders, the HHO method reaches an error threshold with less assembling or solving time than the dG method. The same conclusion is reached on polygonal meshes for the polynomial degree $k = 3$ and both times as well as for $k \in \{0, 1, 2\}$ and assembling time, whereas for $k \in \{0, 1, 2\}$ and solving time, the efficiency of both methods is comparable.

$k = 0$	# DoFs	assembling	solving	$k = 1$	# DoFs	assembling	solving
Morley	65,025	22.9	4.3	HCT	97,283	169.3	19.8
HHO	146,688	275.5	7.0	HHO	244,480	882.0	18.3
C^0-IPDG	65,025	369.5	9.3	C^0-IPDG	130,560	1318.8	27.0

Table 3: Comparison of total DoFs, assembling time, and solving time for the HHO, C^0-IPDG, Morley, and HCT methods. The polynomial degree is chosen so that all the methods in the same column deliver the same decay rates on the H^2-error. Triangular mesh composed of 32,768 cells, 49,408 edges, and 16,641 vertices.

Let us now compare the efficiency of the HHO method to the C^0-IPDG, Morley, and HCT methods on a sequence of successively refined triangulations with 32, 128, 512, 2,048, 8,192, and 32,768 cells. As above, the comparison is made between methods delivering the same decay rates on the H^2-error. This means that the HHO method with polynomial degree $k \geq 0$ is compared with the C^0-IPDG with degree $\ell = k + 2$. Moreover, the HHO($k = 0$) and the C^0-IPDG($\ell = 2$) methods are compared with the Morley element, and the HHO($k = 1$) and the C^0-IPDG($\ell = 3$) methods are compared with the HCT element. Table 3 reports the total number of DoFs, the assembling time, and the solving time for all the methods on the finest triangular mesh. We can see that in the lowest-order case, both the assembling and solving times for the Morley element are (much) smaller than those for the HHO($k = 0$) method, which are, in turn, smaller than those for the C^0-IPDG($\ell = 2$) method. The conclusion for the higher-order case is the same concerning the lower times for HHO($k = 1$) with respect to C^0-IPDG($\ell = 3$), whereas only the assembling time for HCT is (much) smaller than that for HHO($k = 1$), the solving time being instead comparable. One reason for this good performance of HHO compared with HCT can be that the stencil of HCT leads to a more dense system matrix, as a result of the method attaching DoFs to the mesh vertices. Figure 6 reports the error measured in the H^2-seminorm as a function of assembling and solving time, thereby providing a comparison of the efficiency of the various methods

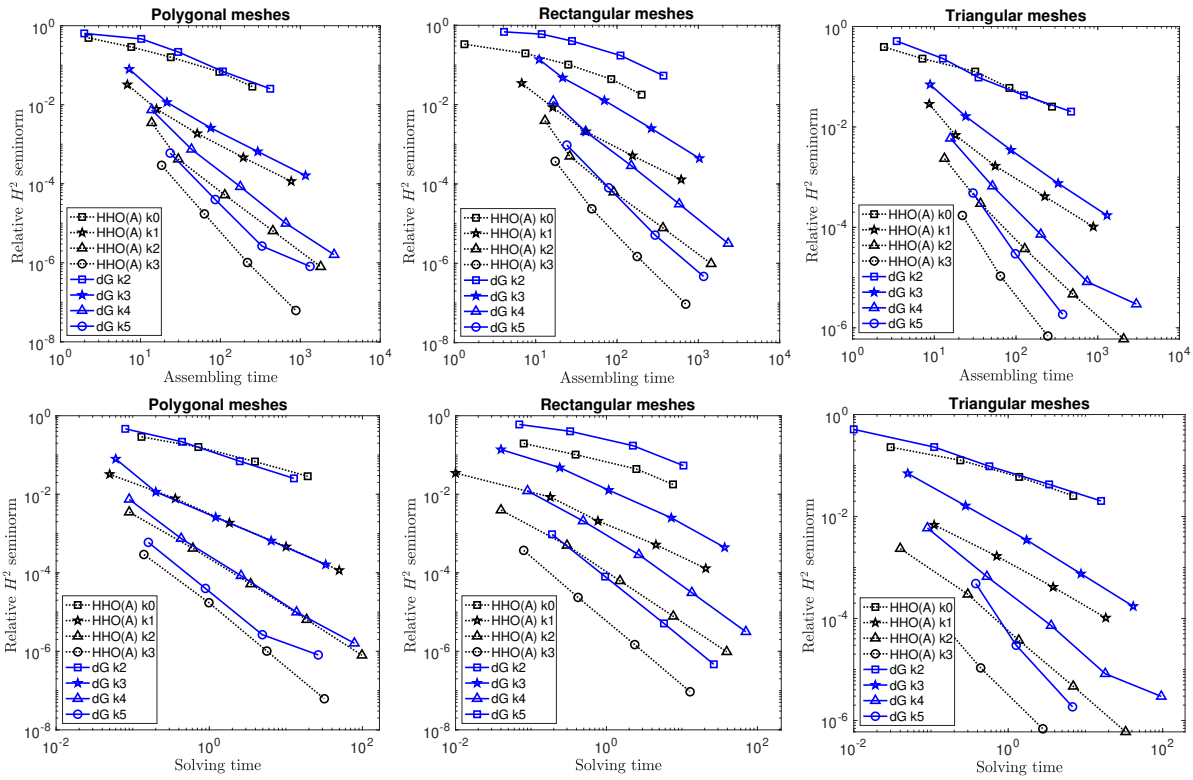

Figure 5: Comparison of HHO and dG methods: relative H^2-seminorm error as a function of assembling time (upper row) and solving time (lower row) on a sequence of polygonal (left), rectangular (center), and triangular (right) meshes and polynomial order $k \in \{0,1,2,3\}$ for HHO and $\ell = k+2$ for dG.

on all the considered triangulations. We notice that the Morley element is the most efficient among the lowest-order methods, whereas the efficiency of the HHO method is better than that of C^0-IPDG, and it is better than that of the HCT element if the solving time is considered, whereas the conclusion is reverted if the assembling time is considered.

7.3 Tests on the HHO-Nitsche method

To conclude, let us briefly illustrate that the proposed HHO-Nitsche (HHO-N) method with a weak enforcement of the boundary conditions performs as well as the HHO method with a strong enforcement of the boundary conditions. We select f and the non-homogeneous boundary data g_D and g_N such that on $\Omega := (0,1)^2$, the exact solution is $u(x,y) = \sin(\pi x)^2 \sin(\pi y)^2 + \exp\left(-(x-0.5)^2 - (y-0.5)^2\right)$. We consider the same sequence of polygonal meshes and the same polynomial degrees as in Section 7.1. Figure 7 presents the relative errors measured in the H^2-seminorm and the L^2-norm using cellwise the reconstruction operator for their evaluation. We compare the HHO and HHO-N methods. Both methods employ the same number of globally coupled DoFs. We can see from Figure 7 that the errors produced by both methods are quite close in all cases.

Acknowledgment

The use of the NEF computing platform at Inria Sophia Antipolis Méditerranée is gratefully acknowledged.

References

[1] M. Abbas, A. Ern, and N. Pignet, *Hybrid High-Order methods for finite deformations of hyperelastic materials*, Comput. Mech., 62 (2018), pp. 909–928.

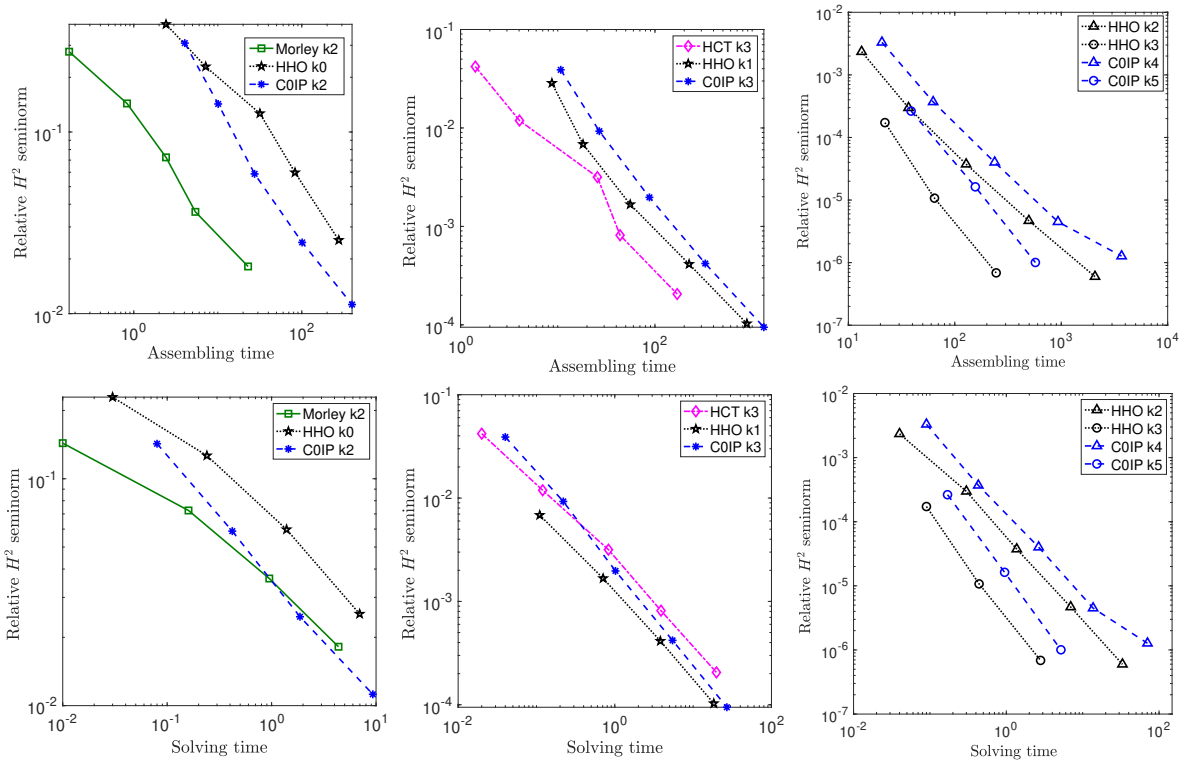

Figure 6: Comparison of HHO, C^0-IPDG, Morley, and HCT methods: relative H^2-seminorm error as a function of assembling time (upper row) and solving time (lower row) on a sequence of triangular meshes.

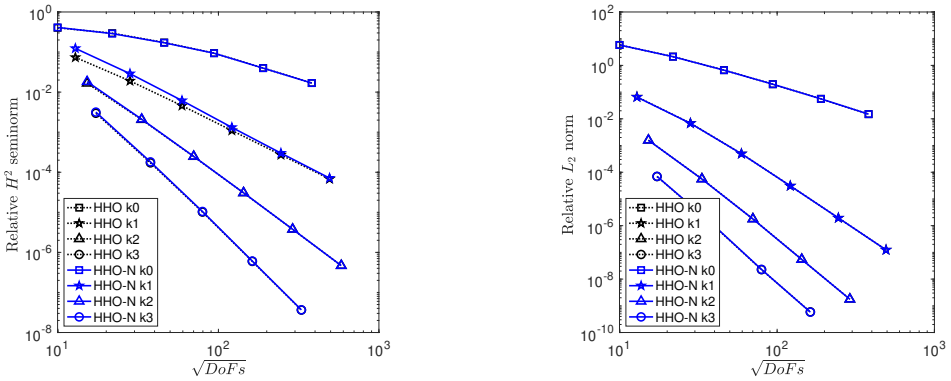

Figure 7: Convergence of HHO and HHO-N methods in H^2- and L^2-(semi)norms on polygonal meshes.

[2] ——, *A Hybrid High-Order method for incremental associative plasticity with small deformations*, Comput. Methods Appl. Mech. Engrg., 346 (2019), pp. 891–912.

[3] P. F. Antonietti, G. Manzini, and M. Verani, *The fully nonconforming virtual element method for biharmonic problems*, Math. Models Methods Appl. Sci., 28 (2018), pp. 387–407.

[4] F. Bonaldi, D. A. Di Pietro, G. Geymonat, and F. Krasucki, *A hybrid high-order method for Kirchhoff-Love plate bending problems*, ESAIM Math. Model. Numer. Anal., 52 (2018), pp. 393–421.

[5] S. C. Brenner and L.-Y. Sung, *C^0 interior penalty methods for fourth order elliptic boundary value problems on polygonal domains*, J. Sci. Comput., 22/23 (2005), pp. 83–118.

[6] F. Brezzi and L. D. Marini, *Virtual element methods for plate bending problems*, Comput. Methods Appl. Mech. Engrg., 253 (2013), pp. 455–462.

[7] E. Burman, M. Cicuttin, G. Delay, and A. Ern, *An unfitted hybrid high-order method with cell agglomeration for elliptic interface problems*, SIAM J. Sci. Comput., 43 (2021), pp. A859–A882.

[8] E. Burman and A. Ern, *An unfitted hybrid high-order method for elliptic interface problems*, SIAM J. Numer. Anal., 56 (2018), pp. 1525–1546.

[9] V. Calo, M. Cicuttin, Q. Deng, and A. Ern, *Spectral approximation of elliptic operators by the hybrid high-order method*, Math. Comp., 88 (2019), pp. 1559–1586.

[10] C. Carstensen and N. Nataraj, *Lowest-order equivalent nonstandard finite element methods for biharmonic plates*, ESAIM Math. Model. Numer. Anal., 56 (2022), pp. 41–78.

[11] F. Chave, D. A. Di Pietro, and S. Lemaire, *A discrete Weber inequality on three-dimensional hybrid spaces with application to the HHO approximation of magnetostatics*, Math. Models Methods Appl. Sci., 32 (2022), pp. 175–207.

[12] G. Chen and M. Feng, *A C^0-weak Galerkin finite element method for fourth-order elliptic problems*, Numer. Methods Partial Differential Equations, 32 (2016), pp. 1090–1104.

[13] C. Chinosi and L. D. Marini, *Virtual element method for fourth order problems: L^2-estimates*, Comput. Math. Appl., 72 (2016), pp. 1959–1967.

[14] F. Chouly, A. Ern, and N. Pignet, *A hybrid high-order discretization combined with Nitsche's method for contact and Tresca friction in small strain elasticity*, SIAM J. Sci. Comput., 42 (2020), pp. A2300–A2324.

[15] P. G. Ciarlet, *The finite element method for elliptic problems*, vol. 40 of Classics in Applied Mathematics, Society for Industrial and Applied Mathematics (SIAM), Philadelphia, PA, 2002.

[16] B. Cockburn, *Static condensation, hybridization, and the devising of the HDG methods*, in Building Bridges: Connections and Challenges in Modern Approaches to Numerical Partial Differential Equations, G. R. Barrenechea, F. Brezzi, A. Cangiani, and E. H. Georgoulis, eds., vol. 114 of Lecture Notes in Computational Science and Engineering, Switzerland, 2016, Springer, pp. 129–178.

[17] B. Cockburn, D. A. Di Pietro, and A. Ern, *Bridging the Hybrid High-Order and hybridizable discontinuous Galerkin methods*, ESAIM Math. Model. Numer. Anal., 50 (2016), pp. 635–650.

[18] B. Cockburn, G. Fu, and F. J. Sayas, *Superconvergence by M-decompositions. Part I: General theory for HDG methods for diffusion*, Math. Comp., 86 (2017), pp. 1609–1641.

[19] D. A. Di Pietro, J. Droniou, and G. Manzini, *Discontinuous Skeletal Gradient Discretisation Methods on polytopal meshes*, J. Comput. Phys., 355 (2018), pp. 397–425.

[20] D. A. Di Pietro and A. Ern, *Mathematical aspects of discontinuous Galerkin methods*, vol. 69 of Mathématiques & Applications (Berlin) [Mathematics & Applications], Springer, Heidelberg, 2012.

[21] ——, *A Hybrid High-Order locking-free method for linear elasticity on general meshes*, Comput. Meth. Appl. Mech. Engrg., 283 (2015), pp. 1–21.

[22] D. A. Di Pietro, A. Ern, and S. Lemaire, *An arbitrary-order and compact-stencil discretization of diffusion on general meshes based on local reconstruction operators*, Comput. Meth. Appl. Math., 14 (2014), pp. 461–472.

[23] D. A. Di Pietro and S. Krell, *A Hybrid High-Order method for the steady incompressible Navier–Stokes problem*, J. Sci. Comput., 74 (2018), pp. 1677–1705.

[24] Z. Dong and A. Ern, *Hybrid high-order method for singularly perturbed fourth-order problems on curved domains*, ESAIM Math. Model. Numer. Anal., 55 (2021), pp. 3091–3114.

[25] G. Engel, K. Garikipati, T. J. R. Hughes, M. G. Larson, L. Mazzei, and R. L. Taylor, *Continuous/discontinuous finite element approximations of fourth-order elliptic problems in structural and continuum mechanics with applications to thin beams and plates, and strain gradient elasticity*, Comput. Methods Appl. Mech. Engrg., 191 (2002), pp. 3669–3750.

[26] A. Ern and J.-L. Guermond, *Finite element quasi-interpolation and best approximation*, ESAIM Math. Model. Numer. Anal. (M2AN), 51 (2017), pp. 1367–1385.

[27] ——, *Finite Elements I: Approximation and Interpolation*, vol. 72 of Texts in Applied Mathematics, Springer Nature, Cham, Switzerland, 2021.

[28] ——, *Finite Elements II: Galerkin Approximation, Elliptic and Mixed PDEs*, vol. 73 of Texts in Applied Mathematics, Springer Nature, Cham, Switzerland, 2021.

[29] ——, *Quasi-optimal nonconforming approximation of elliptic PDEs with contrasted coefficients and H^{1+r}, $r > 0$, regularity*, Found. Comput. Math. (Published online), (2021).

[30] A. Ern and P. Zanotti, *A quasi-optimal variant of the hybrid high-order method for elliptic partial differential equations with H^{-1} loads*, IMA J. Numer. Anal., 40 (2020), pp. 2163–2188.

[31] E. H. Georgoulis and P. Houston, *Discontinuous Galerkin methods for the biharmonic problem*, IMA J. Numer. Anal., 29 (2009), pp. 573–594.

[32] V. Girault and P.-A. Raviart, *Finite element methods for Navier-Stokes equations*, vol. 5 of Springer Series in Computational Mathematics, Springer-Verlag, Berlin, 1986. Theory and algorithms.

[33] P. Grisvard, *Elliptic problems in nonsmooth domains*, vol. 69 of Classics in Applied Mathematics, Society for Industrial and Applied Mathematics (SIAM), Philadelphia, PA, 2011.

[34] C. Lehrenfeld, *Removing the stabilization parameter in fitted and unfitted symmetric Nitsche formulations*, in Proc. of ECCOMAS 2016, 2016.

[35] C. Lehrenfeld and J. Schöberl, *High order exactly divergence-free hybrid discontinuous Galerkin methods for unsteady incompressible flows*, Comput. Methods Appl. Mech. Engrg., 307 (2016), pp. 339–361.

[36] L. Morley, *The triangular equilibrium element in the solution of plate bending problems*, Aero. Quart., 19 (1968), pp. 149–169.

[37] I. Mozolevski and E. Süli, *A priori error analysis for the hp-version of the discontinuous Galerkin finite element method for the biharmonic equation*, Comput. Methods Appl. Math., 3 (2003), pp. 596–607.

[38] L. Mu, J. Wang, and X. Ye, *Weak Galerkin finite element methods for the biharmonic equation on polytopal meshes*, Numer. Methods Partial Differential Equations, 30 (2014), pp. 1003–1029.

[39] ——, *A weak Galerkin finite element method with polynomial reduction*, J. Comput. Appl. Math., 285 (2015), pp. 45–58.

[40] L. Mu, J. Wang, X. Ye, and S. Zhang, *A C^0-weak Galerkin finite element method for the biharmonic equation*, J. Sci. Comput., 59 (2014), pp. 473–495.

[41] C. Schwab, *p– and hp–Finite element methods: Theory and applications in solid and fluid mechanics*, Oxford University Press: Numerical mathematics and scientific computation, 1998.

[42] E. Süli and I. Mozolevski, *hp-version interior penalty DGFEMs for the biharmonic equation*, Comput. Methods Appl. Mech. Engrg., 196 (2007), pp. 1851–1863.

[43] C. Talischi, G. H. Paulino, A. Pereira, and I. F. M. Menezes, *Polymesher: A general-purpose mesh generator for polygonal elements written in Matlab*, Struct. Multidisc. Optim., 45 (2012), pp. 309–328.

[44] A. Veeser and P. Zanotti, *Quasi-optimal nonconforming methods for symmetric elliptic problems. III—Discontinuous Galerkin and other interior penalty methods*, SIAM J. Numer. Anal., 56 (2018), pp. 2871–2894.

[45] ——, *Quasi-optimal nonconforming methods for symmetric elliptic problems. II—Overconsistency and classical nonconforming elements*, SIAM J. Numer. Anal., 57 (2019), pp. 266–292.

[46] R. Verfürth, *Error estimates for some quasi-interpolation operators*, M2AN Math. Model. Numer. Anal., 33 (1999), pp. 695–713.

[47] M. Wang and J. Xu, *The Morley element for fourth order elliptic equations in any dimensions*, Numer. Math., 103 (2006), pp. 155–169.

[48] X. Ye, S. Zhang, and Z. Zhang, *A new P_1 weak Galerkin method for the biharmonic equation*, J. Comput. Appl. Math., 364 (2020), pp. 12337, 10.

[49] R. Zhang and Q. Zhai, *A weak Galerkin finite element scheme for the biharmonic equations by using polynomials of reduced order*, J. Sci. Comput., 64 (2015), pp. 559–585.

[50] J. Zhao, S. Chen, and B. Zhang, *The nonconforming virtual element method for plate bending problems*, Math. Models Methods Appl. Sci., 26 (2016), pp. 1671–1687.

[51] J. Zhao, B. Zhang, S. Chen, and S. Mao, *The Morley-type virtual element for plate bending problems*, J. Sci. Comput., 76 (2018), pp. 610–629.